6-2013

16th Annual SAMPE Student Bridge Contest: Design of a Wood Core Flax Fiber-Reinforced Composite I-Beam

Robert J. Wagner
Union College - Schenectady, NY

16TH ANNUAL SAMPE STUDENT BRIDGE CONTEST

DESIGN OF A WOOD CORE, FLAX FIBER-REINFORCED COMPOSTE I-BEAM

By Robert J. Wagner
Project Advisor: Ronald B. Bucinell, Ph.D., P.E.
MER 498, Senior Project, Design Report
June 12, 2013

Table of Contents

I. Introduction

A composite material is simply a material made up of distinct parts[1]; as such, composites often adapt the desired properties of their individual constituents while abandoning some of their less desired properties. For example, advanced composites such as fiberglass, aramid or carbon fiber composites typically consist of low-density cores, laminated with high-strength reinforcement fibers via a polymer matrix. Such composites adapt the strength properties of their reinforcement fibers while maintaining densities somewhere between those of the three components. The resulting materials have exceptionally high strength-to-weight ratios and are commonly employed in sports equipment, automobiles, boats, the aerospace industry, medical equipment, and military equipment.[2] Despite their high performance standards, traditional advanced composites, such as the ones described, have sustainability, manufacturing and cost issues.

Between fiberglass, aramids, and carbon fibers, fiberglass is the least costly reinforcement fiber to use because it is silica-based and requires relatively little energy to manufacture.[3] However, fiberglass has the highest densitiy of the three fiber categories, in the range of 90.2 kg/m^3 to 2,570 kg/m^3.[4] Aramids, have considerably lower densities from 52.1 kg/m^3 to 1,440 kg/m^3, but are synthetic and polymer-based; thus they are non-renewable and more expensive to manufacture than fiberglass.[4,5] Carbon fibers are slightly more dense than aramids with densities ranging from 64.9 kg/m^3 to 1,800 kg/m^3, but have the highest strength-to-weight ratios of the three traditional reinforcement fibers.[4] They, like aramids, are polymer-based though; therefore, they too are non-renewable, and expensive to produce.[6] The core and bonding matrix materials used in conjunction with these reinforcement fibers share similar disadvantages. Common low-density core materials such as polystyrene foam, although not expensive to manufacture, are also made from non-renewable polymers, are rarely recycled, and do not biodegrade. In fact, polystyrene foam accounts for 25-30 % of landfills by volume.[7] Finally, typical bonding matrices are commonly made from polymer-based epoxies which are non-renewable and if not properly disposed of, can harm the environment.[8,9] When all three components of high-performance composites are brought together, they form materials that will not biodegrade and may not be recycled without greatly depreciating mechanical properties.[10] For all these reasons, it is worthwhile considering the substitution of

traditional advanced composite materials with sustainable materials whose mechanical properties may not exactly match those of traditional constituents, but whose lower costs and environmental benefits outweigh the sacrificed strength.

Potential sustainable composite substitutes include natural reinforcement fibers, natural core materials, and polymer resins from natural oils. Natural reinforcement fibers could come from plant matter such as pineapples hides, bananas peels, bamboo stems, hemp stems, flax stems, etc. Natural core materials could be made from lightweight woods such as balsa wood or poplar plywood. Natural core materials could also be made from mycelium (fungal fibers) grown into desired geometries by the company Ecovative Design.[11] Polymer resins made from natural resins are difficult to acquire, but institutions such as Rensselaer Polytechnic Institute are currently working to develop such materials. The natural and renewable nature of these alternatives would make them cheaper than traditional materials due to their availability. Such materials could also be made to biodegrade after their useful or intended lifespan; therefore they would not contribute to long-term waste storage or recycling demands.

The goal of this project was to demonstrate the applicability of natural composites in structural applications for objects with shorter intended life spans such as sports equipment. This was done by competing in the 16th Annual SAMPE Student Bridge Contest with a natural fiber, natural core composite I-beam in Long Beach, California on May 8th, 2013. The beam was to withstand 3,000 lbs under three-point-bending while maintaining a low weight. In order to compete, natural reinforcement fibers, natural core materials and a bonding matrix had to be identified; a beam within allowable contest dimensions had to be designed; and a feasible manufacturing process had to be developed and carried out. This report details the progression of the project and present its results by first offering some background on fiber-reinforced composite materials, their basic constituents and their manufacturing processes. It then provides some design specifications for the SAMPE Student Bridge Contest and a feasibility discussion of said specifications and potential manufacturing processes. Finally, the report will discuss the three beams made during this project, offer information on the competition beam's performance and some recommendations for next year's competition.

II. Background

The following content will examine the way in which beams were loaded in the SAMPE Student Bridge Contest. It will then compare the ultimate tensile strengths and elasticity of various natural and synthetic fibers to justify selection of the materials used, and describe the fiber reinforcements purchased. It will then identify which types of stresses develop in which sections of a beam under competition loading conditions, the resulting failure modes liable to occur, and how such failure modes are typically avoided in composite designs. The section will end by examining a manufacturing process called vacuum bagging that evenly applies pressure to composites during curing, in order to reduce their porosity.

The loading scenario for the SAMPE Student Bridge Contest, natural fiber I-beam category is as shown in **Figure 1**. The beam was to be simply supported by two 1 inch diameter rods, spaced 23 inches apart, and centrically loaded using a 4 inch by 4 inch loading cell. Each natural fiber I-beam was meant to withstand 3,000 lbs of loading, which over a 4 inch length translates to a distributed load of 750 lbs/in. Beams under such loading conditions often fail under tension in their bottom flanges, or compression in their top flanges. Since the reinforcement fibers in a composite are primarily responsible for carrying tensile loads, the first step to designing a competition beam is selecting suitable natural fiber reinforcements. Literature searches were conducted regarding the mechanical properties of various natural plant fibers. The primary mechanical properties of concern were tensile yield stress and ultimate tensile stress, which characterize the fibers ability to carry tension. The elastic (Young's) modulus, which characterizes stiffness, was also researched. **Table 1** documents the mechanical properties of various natural fibers, E-glass fibers (a commonly used glass fiber), Kevlar 29 (a commonly used aramid fiber) and carbon fibers, according to a variety of sources.

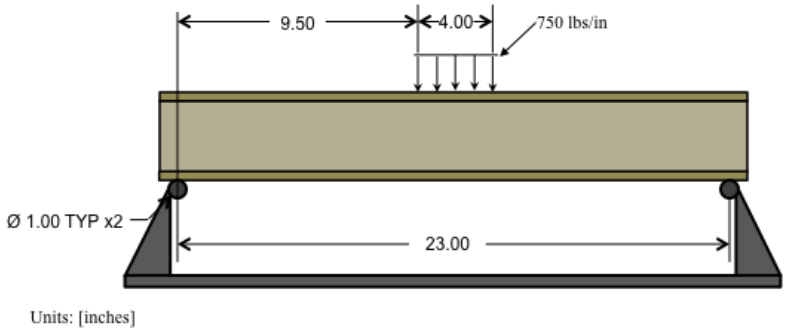

Figure 1. A side view of the SAMPE Student Bridge Contest, natural fiber I-beam loading scenario is shown.

Table 1. Yield stresses, ultimate tensile strengths and elastic modulus of various natural fibers are recorded as available. Ultimate tensile strength and elastic modulus are given for E-glass fibers, Kevlar 29, and carbon fibers for comparison.

Fiber Type	Yield Stress, σ_y (MPa)	Ultimate Tensile Strength, σ_{ult} (MPa)	Elastic Modulus, E (GPa)
coconut fiber[12]	25-34	68	0.5-2
pineapple fiber[13]			2.76
hemp fiber[14,15,16]		300-800	30-60
jute fiber[16]		200-500	20-55
flax fiber[16]		500-900	50-70
bamboo fiber[17]		10.3	414.5
E-glass fiber[18]		2,000	80
Aramid (Kevlar 29)[19]		2,920	70.5
carbon fiber[20]		3,500	138

It is clear from **Table 1** that natural fibers are universally weaker and stretch more (excluding bamboo) under tension than commonly used synthetic fibers; however their tensile strengths are still relatively high. Amongst the natural fibers, flax fibers were identified as the most suitable fiber reinforcements due to their high ultimate tensile strengths in the range of 500-900 MPa (72.5-130.5 ksi) and relatively high elastic modulus values in the range of 50-70 GPa (7,250-101,530 ksi).

A Belgian company, LINEO, sells a product called FLAXPREG, which is a flax fiber fabric impregnated with epoxy. Such fabrics are referred to as pre-pregs. The epoxy in a pre-preg is a partially cured thermoset, which prevents the epoxy from running out of the fabric. Two types of FLAXPREG purchased from LINEO are shown in **Figure 2**.

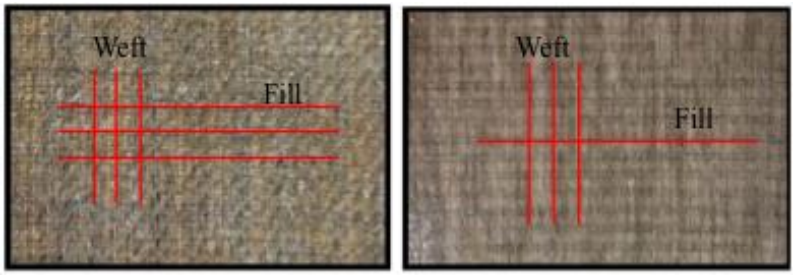

Figure 2. Left: Basic FLAXPREG 150g/sqm. **Right:** Unidirectional FLAXPREG 150 g/sqm.

Five meters of balanced fabric (BL) FLAXPREG and five meters of unidirectional (UD) FLAXPREG, each with a sheet density of 150 g/m^2, were purchased. The BL fabric contains roughly 50 % of its fibers in its primary weave (weft) direction and 50 % of its

fibers in its secondary weave (fill) direction. The UD fabric contains nearly all of its fibers in its weft direction and contains only a few fibers in its fill direction in order to hold the fabric together. The wefts and fills of each type of fabric are highlighted in **Figure 2**. Each pre-preg is 50 % thermoset epoxy by volume.[21] By purchasing FLAXPREG, both the reinforcement fibers and the bonding matrix for the beam were acquired. However, core materials remained to be selected.

The core of an advanced composite part is meant to provide its shape, but for the SAMPE competition the beam's core needs to withstand high compression loading imparted by the loading apparatus's rod supports. Mycelium cores were not selected due to their low crushing strengths. Instead, poplar plywood and balsa wood were identified as suitable core materials for their high strength-to-weight ratios and compressive strengths. Once all materials were selected the design process of the beam was initiated by considering load distributions in a beam under competition loading conditions.

In order to design a load bearing, fiber-reinforced composite, one must consider where tensile, compressive, and shear stresses develop. A beam under competition loading conditions will develop normal tensile and compressive stresses – stresses in the direction of the *z*-axis – as shown in **Figure 3**.

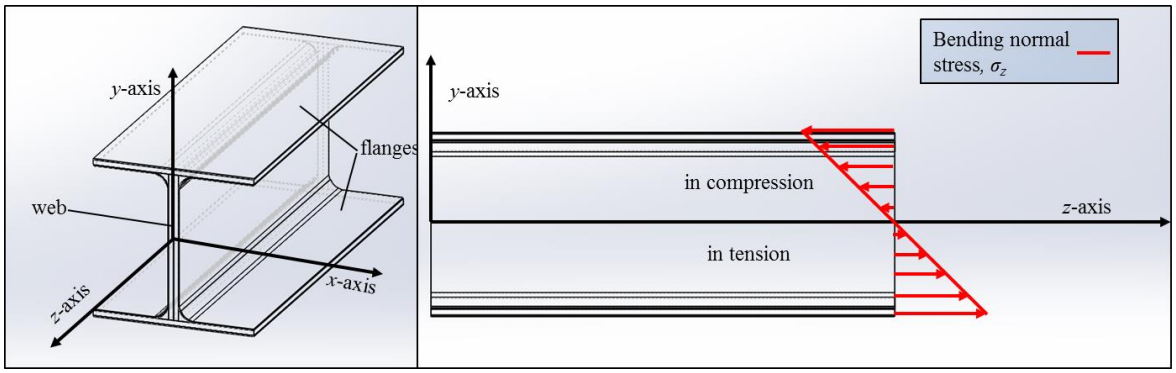

Figure 3. Left: The *x*-axis, *y*-axis and *z*-axis of the beam, as referenced for the remainder of this report, are shown with respect to an arbitrary I-beam. **Right:** Bending normal stress distribution is shown as a function of *y* for a beam under competition loading conditions.

The directional convention used in the remainder of this report is illustrated in the left image, of a sectioned view of a beam, in **Figure 3**. The *xz*-plane is located midway up the beam. The right image in **Figure 3** shows how bending normal stresses (σ_z) – or compressive and tensile stresses in the *z* direction – will develop and vary with *y*-position. For a beam that is symmetrical about the *xz*-plane, the neutral surface, or

surface where no bending normal stresses develop, is simply the *xz*-plane. Maximum compression and tension for a beam under competition loading conditions will develop at the *y* positions furthest away from the neutral surface or when *y* is plus or minus half of the beam height. Shear stresses, in a beam undergoing bending due to loads applied in the *y* direction, will develop in the direction of the *y*-axis and *z*-axis and are primarily carried by the web. The nature of these shear stresses is illustrated in **Figure 4**, which isolates an infinitesimal element of a beam undergoing an arbitrary shear force, *S*. The beam if fixed at one end.

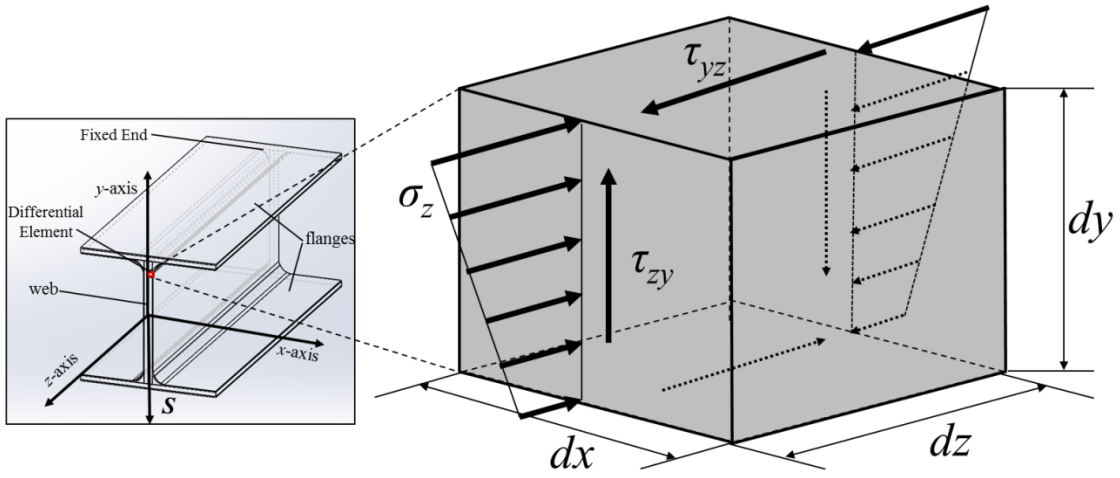

Figure 4. Left: A cantilever beam is shown with a shear force, *S*, acting on its free end in the negative *y* direction. **Right:** An infinitesimal beam element is shown in static equilibrium with bending normal stresses on the faces normal to the *z*-axis and shear stresses on the faces normal the *z*-axis and *y*-axis.

If the beam remains in static equilibrium, then the forces and bending moments acting on any element of it must sum to zero. A shear stress develops on the positive *z*-face in the positive *y* direction (denoted by τ_{zy} in **Figure 4**) is counteracted by a shear stress of equal magnitude that develops on the negative *z*-face in the negative *y* direction (shown as a dotted arrow in **Figure 4**). The equal, but opposite nature of these stresses imparts a moment on the element (M_x) given by;

$$M_x = (\tau_{zy} dx dy) dz$$

Where $\tau_{zy} dx dy$ is the shear force, and dz is the moment arm. In order to counteract said moment, shear forces develop on the *y* faces of the element and are parallel to the *z*-axis. For infinitesimal beam elements, these forces are essentially equal in magnitude and induce equal and opposite shear stresses denoted by τ_{yz} and a dotted arrow in **Figure 4**. Since no shear stress can develop on the top face of the beam, it can be resolved that the

shear stresses on either *y*-face of a given element (with the exception of those at the neutral surface) are not equal, otherwise no such stresses could develop anywhere in the beam. In fact, for a beam under competition loading conditions that is symmetrical about the *xz*-plane, maximum shear stress develops at the neutral surface where *y* is equal to zero.[21] In reality, for composite materials whose material properties are anisotropic and heterogeneous, the internally developed normal and shear stresses will not necessarily behave according to the background and analysis in this report. However such analysis is still useful in realizing that the maximum bending normal stresses are carried by the flanges in an I-beam and maximum shear stresses are carried by the web.

In order to prevent failure due to maximum bending normal stresses and shear stresses, reinforcement fibers in the flanges and web of an I-beam should be oriented at different angles. **Figure 5** shows how different fiber orientations are referenced with respect to the *z*-axis for the remainder of this report.

Figure 5. Left: BL fabric at 0° (weft is parallel to the z-axis). **Center:** BL fabric at 45°. **Right:** BL fabric at 90° (weft is orthogonal to the *z*-axis).

The 0°, 45° and 90° reference angles shown in **Figure 5** are all with respect to the *z*-axis and apply to both BL and UD FLAXPREG. Tensile and compressive loads are best carried by 0° fibers as shown in the far left image of **Figure 5**; therefore, plies of UD fabric at 0° should be included in the flanges of an I-beam under competition loading conditions. Shear loads are best carried by 45° fibers; therefore, plies of BL fabric at 45° should be included in the web of an I-beam under competition loading conditions. Since the core material in an I-beam's web will also carry shear effectively, very little 45° BL fabric needs to be included in the web. However, in order to maintain symmetry and prevent twisting, at least two plies of 45° BL fabric, with alternating weft orientations, should be included on each side of such a web.

Many failure modes exist for fiber-reinforced composites that are not necessarily addressed by orienting the fibers properly. Problems such as dewetting (caused by poor bonding between the fibers and epoxy matrix), micro tears of the reinforcement fibers, delamination (separation of reinforcement layers) and problems associated with high matrix porosity can all cause premature mechanical failure. Dewetting is a common problem when attempting to bond hydrophilic natural fibers to hydrophobic thermoset resins. Dewetting is addressed by LINEO's patented fiber treatment and thermoset impregnation processes. LINEO's process also ensures that the flax fibers will not absorb moisture once impregnated as well.[22] Micro tears of the flax fibers are unavoidable, but the effects become negligible if the thermoset resin is properly bonded to the fibers. This is because, as illustrated in **Figure 6**, when a micro tear occurs (Step 1), equal and opposite shear loads develop at the fiber-matrix interface (Step 2).

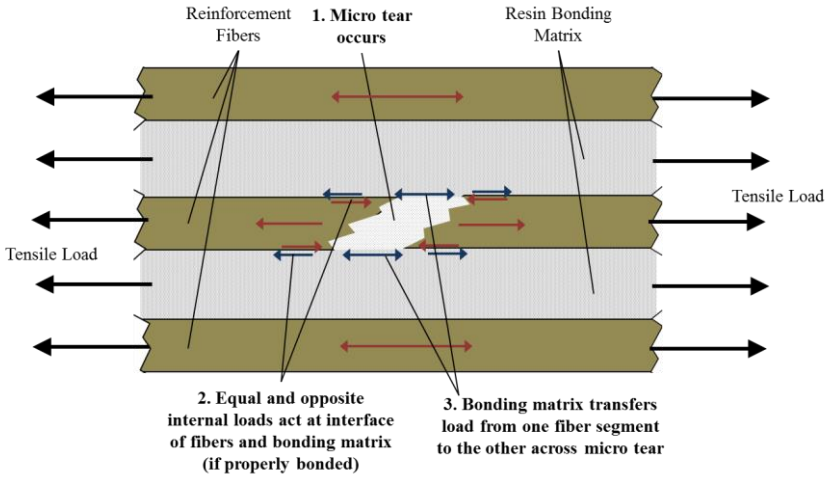

Figure 6. The mechanism by which loads are transferred across micro tears is shown.

The bonding matrix then carries the load to the other side of the micro tear (Step 3 in **Figure 6**) and transfers load back into the fiber. Essentially, a properly bonded resin will transfer loads from one fiber segment to the next, effectively bypassing any micro tears that develop. Other problems such as composite porosity can be decreased by properly applying pressure to all of the outer surfaces of the beam during the curing of the thermoset. This is achieved by a composite manufacturing process called vacuum bagging for which the steps are described in the following paragraphs.

Vacuum bagging allows for even pressure distribution along the outer surfaces of composites during curing, thereby ensuring the development of proper bonds between the core and fabric plies (defined by the absence of air pockets between layers and low porosity). The process of vacuum bagging, illustrated in **Figure 7**, requires that the

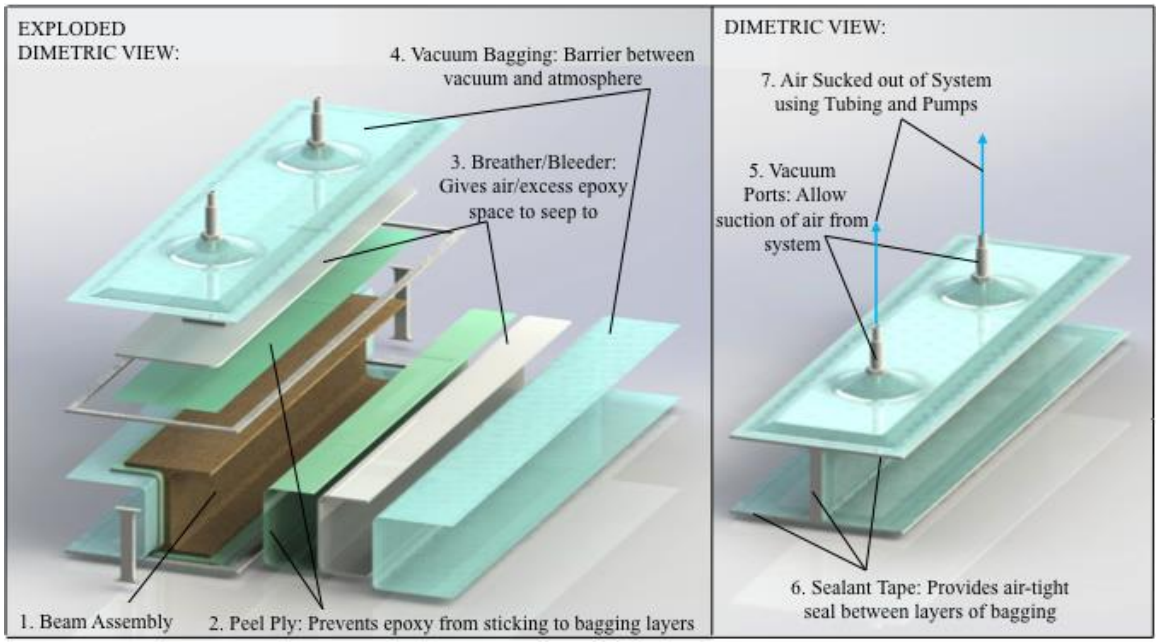

Figure 7. Steps 1 through 7 of the vacuum bagging process are illustrated.
<Image created using SolidWorks Education Edition>

composite assembly be wrapped in several layers of material. Once all laminates are in place, the composite assembly is wrapped in a layer of nylon peel ply fabric to prevent the thermoset from bonding to any of the other bagging layers (see Step 2 in **Figure 7**). Then the assembly is wrapped in a breather/bleeder layer that serves two purposes. The breather/bleeder allows air to be evenly sucked out of the system, and gives excess resin somewhere to seep during vacuum bagging (see Step 3 in **Figure 7**). Next the assembly is wrapped in non-porous nylon bagging which will provide an airtight layer (see Step 4 in **Figure 7**). Incisions are made in the nylon bagging and plastic vacuum ports are placed such that the bagging locks between the base of the ports, and threaded plastic nuts on the ports. Rubber o-rings are located on the vacuum ports to maintain an airtight seal at the junction of the nylon bagging and the ports. Once the vacuum ports are in place the edges of the nylon bagging are sealed airtight to one another using grey sealant tape. Air between the bagging and the composite assembly is then sucked out, via plastic

tubing and air pumps, until vacuum is attained (see Steps 5 and 6 in **Figure 7**). As illustrated in **Figure 8**, this creates an atmospheric pressure differential between the inner and outer surfaces of the bagging. Consequently, the bagging evenly distributes pressure over the entire surface of the beam. Vacuum bagging is advantageous for its ability to apply pressure to otherwise difficult to reach places, such as the inner corners of an I-beam (**Figure 8**).

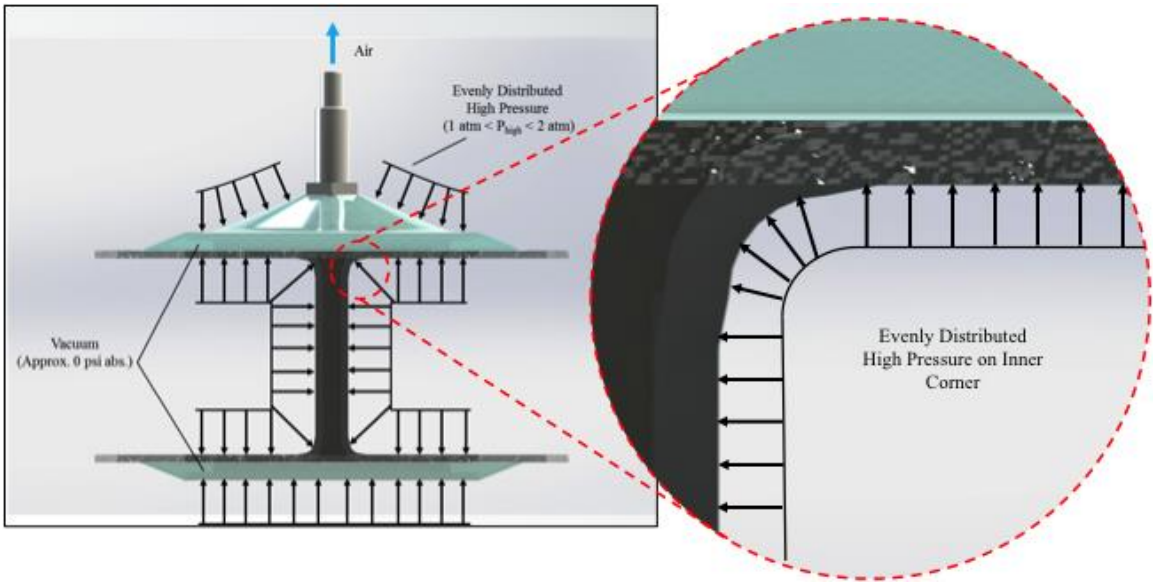

Figure 8. Once air is evacuated from the vacuum bagging system, pressure is evenly distributed over the outer surfaces of the beam.

Proper vacuum bagging ensures that no air pockets exist between layers of fiber reinforcements and insures against high porosity. However, in order to cure the thermosets, heat must be applied to the system. This is often accomplished by using an autoclave. The autoclave in the Union College manufacturing facility, shown in **Figure 9**, was used for this project. In order to vacuum

Figure 9. Union College Manufacturing Lab Autoclave.

bag a composite in an autoclave, the vacuum bagging process must be carried out outside of the autoclave. Then, as seen in **Figure 10**, a valve must be used to close off the system temporarily while maintaining an airtight seal and vacuum (Step 8 of **Figure 10**). The entire assembly must then be moved into the autoclave, and reconnected to a tubing system and pump (Step 9 of **Figure 10**).

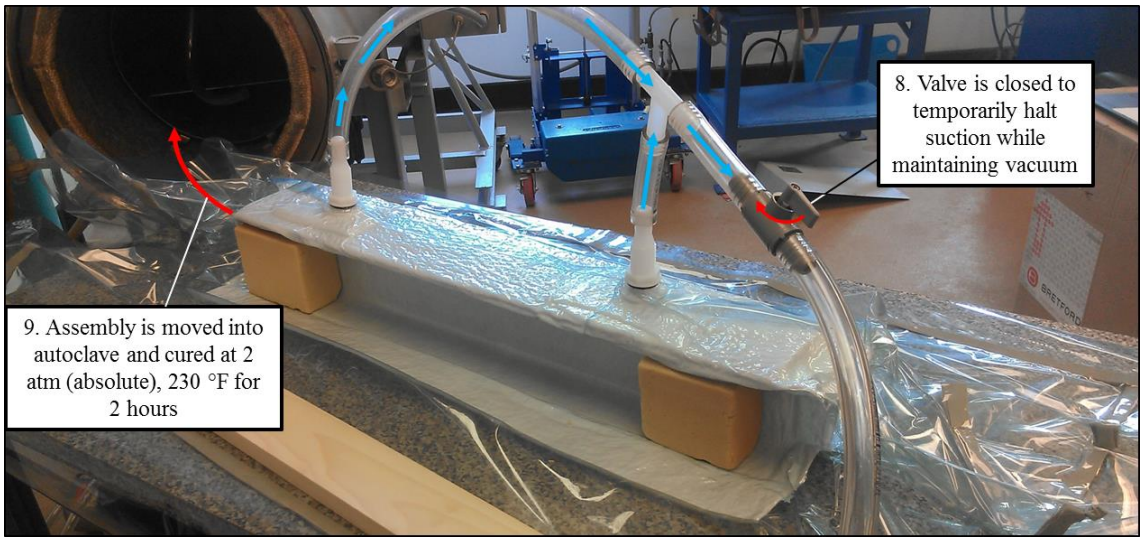

Figure 10. The eighth and ninth steps of the vacuum bagging process are shown.

Then suction of the air may be resumed, and the autoclave may be closed and set to a higher temperature and pressure.

Prior to designing and manufacturing the beam, information was gained about the competition loading conditions, which materials are most suitable for a natural fiber composites, how different stresses are carried in a beam under competition loading conditions, how to address said stresses, and how to effectively manufacture composites. FLAXPREG, balsa wood and poplar plywood were selected as appropriate beam materials based on their strength properties and availability. It was determined that the flanges in a competition beam primarily carry bending normal stresses and the webs primarily carry shear forces. In order to prevent failure due to bending normal stresses and shear stresses, the fiber reinforcements in FLAXPREG should be oriented at 0° and 45° with respect to the *z*-axis, respectively. The manufacturing process of vacuum bagging was examined and identified as a suitable way to produce the final composite I-beam. The following section details the analysis and considerations undergone in order to design a competition beam based on the knowledge gained.

III. Design Specifications

This section presents the analysis undergone in order to provide a sufficiently strong competition beam of suitable dimensions. First, the competition loading scenario is briefly reexamined and allowable beam dimensions of each beam are provided. Then the necessary moments of inertia of exclusively 0° UD FLAXPREG about the *x*-axis, that would prevent failure due to two failure modes, are determined.

As shown earlier in **Figure 1**, during the SAMPE competition, the beam is simply supported on two 1-inch diameter rods spaced 23 inches apart. The beam is then vertically loaded with up to 3,000 lbs at the center of its top flange using a 4-inch by 4-inch loading block. Beams are scored based on the weight they carried up to 3,000 lbs. Any load carried after 3,000 lbs does not factor into the score. If two or more beams carried 3,000 lbs, the beam that weighed the least was taken as the winner. The competition rules also constrain the dimensions of the beam. Each I-beam has to be at least 24 inches long and cannot exceed the dimensions illustrated in **Figure 11**. The cross-sectional dimensions of the beam do not need to be uniform along the length of the beam; however, the beam may never be more that 4 inches wide, or 4 inches tall, and the web cannot be greater than 0.6 inches thick. Finally, there must always be a gap between the two flanges of the beam.

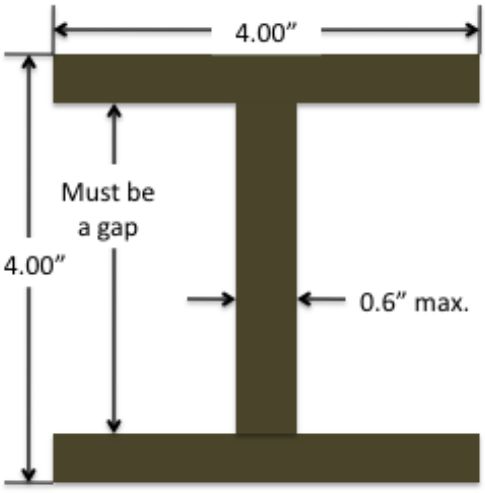

Figure 11. The maximum allowable cross-sectional dimensions of the beam according to competition rules are shown.

According to the loading scenario in **Figure 1**, the maximum load to be carried by each beam is an evenly distributed load of 750 lbs/in acting over the middle 4 inches of the top surface of the beam. A free body diagram of the loading scenario is shown in **Figure 12(a)**. Since the beams will remain in static equilibrium, reaction forces from the supports will act on the bottom surface of the beam and can be modeled as point loads. Due to the symmetrical nature of the loading, and force equilibrium of the beam, said reaction forces will each be 1,500 lbs. Internal reaction loads will develop in the beam

due to the loading scenario. Said internal loads consist of shear forces, and bending moments. As shown in **Figures 12(b)**, **12(c)** and **12(d)**, cuts were made between the locations at which the beam undergoes abrupt loading changes (labeled **A**, **B**, **D** and **E**). Either the right or left side of the cut beam was then used to develop a new free body diagram, containing the internally developed shear force (*V*) and the internally developed bending moment (*M*).

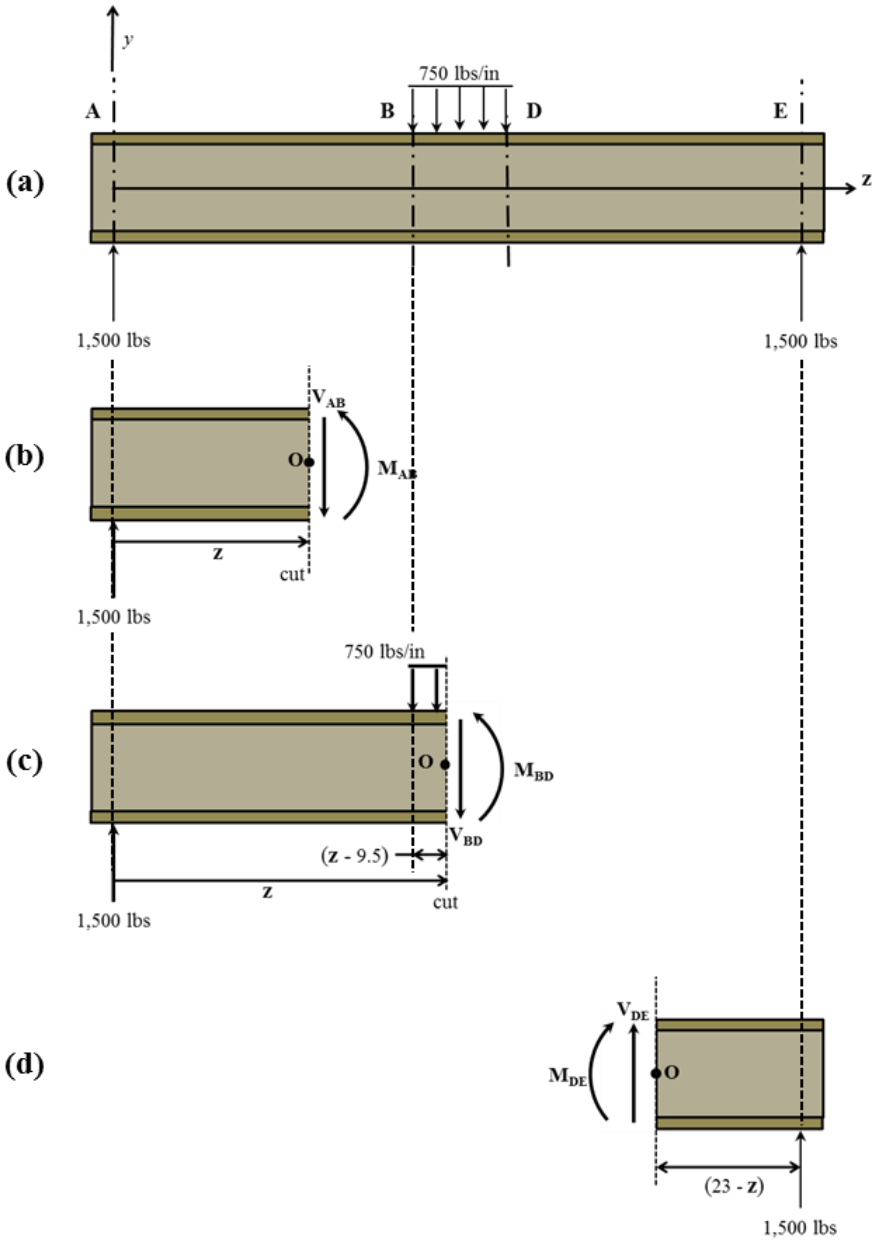

Figure 12. (a) A free body diagram of the beam is shown with labeled axes. **(b)** A cut was made between **A** and **B** and a free body diagram of the beam to the left of the cut is shown. **(c)** A cut was made between **B** and **D** and a free body diagram of the beam to the left of the cut is shown. **(d)** A cut was made between **D** and **E** and a free body diagram of the beam to the right of the cut is shown.

The free body diagrams were then used to conduct force equilibrium and bending moment equilibrium analyses, which respectively state that the sum of all forces and the sum of all moments about some point, *O*, are equal to zero;

$$\sum F = 0 \qquad \textbf{(1)}$$

$$\sum M_o = 0 \qquad \textbf{(2)}$$

Use of **Equations 1** and **2** allowed *V* and *M* to be found as functions of the longitudinal distance away from the left support in **Figure 11(a)**, or *z*. For example, **Equation 1** for section BD of the beam is as follows;

$$+\uparrow \sum F_y = 0 = 1{,}500 - 750(z - 9.5) - V_{BD} \text{ [lbs]}$$

Solving for $\boldsymbol{V_{BD}}$ gives;

$$V_{BD} = -750z + 8{,}625 \text{ [lbs]}$$

Equation 2 for section BD of the beam about point *O* is as follows;

$$\circlearrowleft + \sum M_o = 0 = 750(z - 9.5)\left(\frac{z-9.5}{2}\right) - 1{,}500z + M_{BD} \text{ [in*lbs]}$$

Solving for M_{BD} gives;

$$M_{BD} = -375z^2 + 8{,}625z - 33{,}843.75 \text{ [in*lbs]}$$

Such analysis provides the following equations for *V* and *M* in the three beam sections;

$$V_{AB} = 1{,}500 \text{ [lbs]} \qquad \textbf{(3)}$$

$$V_{BD} = -750z + 8{,}625 \text{ [lbs]} \qquad \textbf{(4)}$$

$$V_{DE} = -1{,}500 \text{ [lbs]} \qquad \textbf{(5)}$$

$$M_{AB} = 1{,}500z \text{ [in·lbs]} \qquad \textbf{(6)}$$

$$M_{BD} = -375z^2 + 8{,}625z - 33{,}843.75 \text{ [in·lbs]} \qquad \textbf{(7)}$$

$$M_{DE} = 34{,}500 - 1{,}500z \text{ [in·lbs]} \qquad \textbf{(8)}$$

Equations 3 through **5** are plotted in **Figure 13** from $0 \leq z \leq 23$ inches. **Figure 13** reveals that the maximum internal shear force developed in the beam (V_{max}) is 1,500 lbs and it occurs between the supports and the loading block.

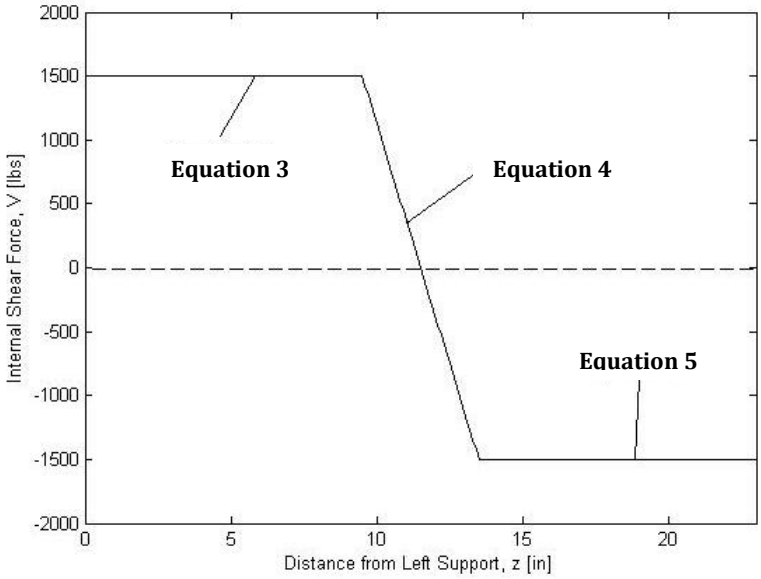

Figure 13. Internal shear force in the beam is plotted with respect to distance from the left support of the loading apparatus.

Equations 6 through **8** are plotted in **Figure 14** from $0 \leq z \leq 23$ inches. **Figure 14** reveals that the maximum bending moment developed in the beam (M_{max}) occurs at the middle section of the beam (where z equals 11.5 inches) and has a value of 15,750 in·lbs.

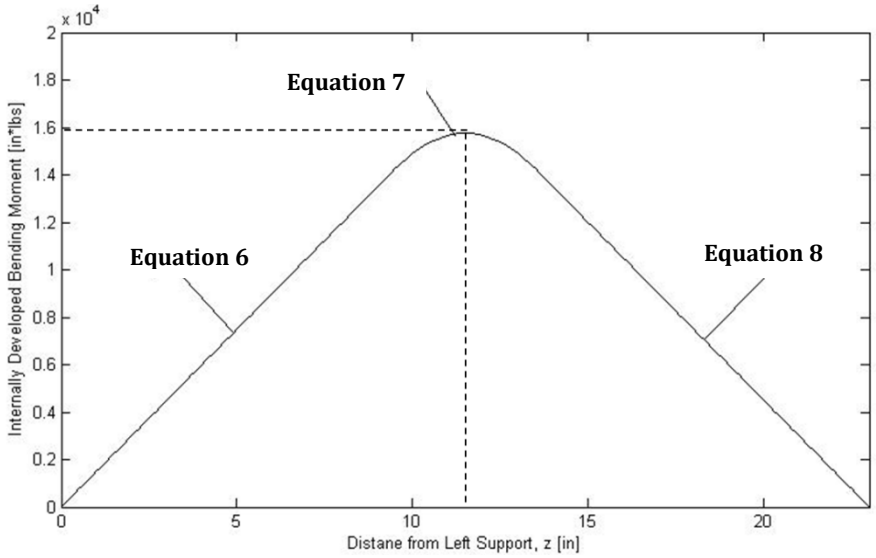

Figure 14. Internally developed bending moment in the beam is plotted with respect to distance from the left support of the loading apparatus.

After identifying the maximum shear forces and bending moments in the beam and where they occur, optimum beam geometry could be determined to minimize material and weight while still avoiding failure. In order to determine suitable beam

geometry two failure criteria provided by SAMPE had to be examined. The failure criteria are as follows;

1. The beam must not fail catastrophically.
2. Maximum beam deflection must not exceed more than 1 inch.

Catastrophic failure is prevented by ensuring that the maximum normal stresses and shear stresses in the beam do not exceed the ultimate normal stress and ultimate shear stress of the materials used. However, this can be difficult for anisotropic materials such as FLAXPREG, whose properties vary along different axes and planes. Furthermore, failures of composite materials are complicated by phenomena such as delamination, micro tears in the fibers and other problems. For simplicity's sake, the following analyses address only the maximum bending normal stresses – specifically tensile stresses – developed in the longitudinal axis (*z*-direction) of the beam.

In general, bending normal stress (σ_z) for a beam is given by;

$$\sigma_z = \frac{My}{I_{xx}} \qquad \textbf{(9)}$$

Where M is the applied bending moment, y is distance away from the neutral axis – the axis at which bending normal stress is zero – and I_{xx} is the first moment of area of the beam's cross section about the x-axis. From **Equation 9**, it is apparent that increasing M and y will decrease σ_z and decreasing I_{xx} will increase σ_z. Therefore, assuming I_{xx} is kept constant (or that the cross section is uniform) with respect to z, the maximum bending normal stress ($\sigma_{z,max}$) is given by;

$$\sigma_{z,max} = \frac{M_{max}y_{max}}{I_{xx}} \qquad \textbf{(10)}$$

Where M_{max} is the maximum bending moment developed in the beam and y_{max} is the furthest distance of beam material away from the neutral axis at the cross section where M_{max} occurs. Failure occurs when $\sigma_{z,max}$ exceeds the ultimate tensile strength of the material (σ_{ult}); therefore, if M_{max} and y_{max} are known, and σ_{ult} is substituted into **Equation 10** for $\sigma_{z,max}$, then one can solve for the minimum first moment of area needed in order to prevent failure due to tension. This is expressed below in **Equation 11**;

$$I_{xx,tens} = \frac{M_{max}y_{max}}{\sigma_{ult}} \qquad \textbf{(11)}$$

Where M_{max} is 15,750 in·lbs, y_{max} is 2 inches (due to the dimensional constraints of the competition) and σ_{ult} is 47,860 psi[18].

Substituting values into **Equation 11** gives;

$$I_{xx,tens} = \frac{(15{,}750\ \text{in*lbs})(2\ \text{in})}{\left(47{,}860\ \frac{\text{lbs}}{\text{in}^2}\right)}$$

Therefore;

$$I_{xx,tens} = 0.658\ \text{in}^4$$

Presumably, if the 0° UD FLAXPREG in the beam can withstand competition loading on its own, then the entire beam (including BL FLAXPREG and core materials) could withstand competition loading. Therefore, in order to prevent failure due to tension in the bottom flange of the beam, the I_{xx} of all 0° UD FLAXPREG in the beam should be kept above 0.658 in^4.

In order to analyze the maximum deflection (δ_{max}) of the beam when loaded with 3,000 lbs, the applied load (P) and reaction loads can be modeled as a point loads such that the free-body-diagram becomes what is shown in **Figure 15**. The deflection of a composite beam under such loading conditions is complicated by its anisotropic and heterogeneous nature. However, for an isotropic, homogenous beam under competition loading conditions, the maximum deflection is given by;

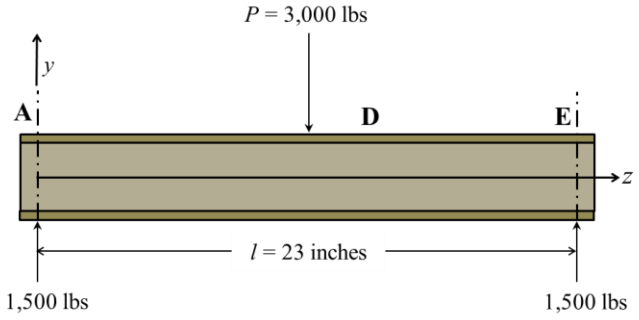

Figure 15. A free body diagram of the beam is shown with the applied load modeled as a point load.

$$\delta_{max} = \frac{Pl^3}{48EI_{xx}} \qquad \textbf{(12)}^{[19]}$$

Where l is the distance between supports (23 inches) and E is the elastic modulus of the material (5,076 ksi for UD FLAXPREG along its weft direction). By isolating I_{xx} in **Equation 12**, one can solve for the minimum allowable value of I_{xx} allowed in order to prevent deflection of 1 inch or greater. Isolating I_{xx} in **Equation 12**, gives;

$$I_{xx,def} = \frac{Pl^3}{48E\delta_{max}} \qquad \textbf{(13)}$$

Substituting in all known values and the elastic modulus of UD FLAXPREG gives;

$$I_{xx,def} = \frac{(3{,}000\text{lbs})(23\text{in})^3}{48(5{,}076{,}320\text{psi})(1\text{in})}$$

Therefore;

$$I_{xx,def} = 0.150 \text{ in}^4$$

As before, if the 0° UD FLAXPREG alone could prevent 1 inch deflection, then it stands to reason that the 0° UD FLAXPREG coupled with the other constituents of the beam could prevent 1 inch deflection. In order to prevent failure due to 1 inch deflection of the beam, the I_{xx} of all 0° UD FLAXPREG in the beam should be kept above 0.150 in^4. However, in reality deflection of composites is liable to involve less predictable, asymmetrical deflections and twisting. Regardless of complications from anisotropy, since $I_{xx,tens}$ is greater than $I_{xx,def}$, failure due to tension is the critical failure mode and the beam was designed such that I_{xx} of 0° UD FLAXPREG (alone) exceeded 0.658 in^4. Three beams were made during the course of this project and it was ensured for each beam that $I_{xx,UD}$ exceeded 0.658 in^4. In the following section the feasibility, of making beams that adhere to the necessities dictated in this section, is examined.

IV. Feasibility Discussion

This section examines the feasibility of manufacturing a beam from the selected materials whose first moment of inertia, of solely 0° UD FLAXPREG, is greater than or equal to 0.658 in^4, and whose dimensions do not exceed those specified by the competition rules. It also examines the feasibility of vacuum bagging an I-beam and heating it in Union College's Manufacturing Facility's autoclave.

The beam dimensions specified by SAMPE are manageable, as the minimum allowable length of a beam is merely 24 inches and the allowable cross sectional dimensions may not exceed 4 inches by 4 inches. The autoclave used in this project is amply suited to accommodate beams of such dimensions, even once they are dressed with vacuum bagging materials. Five square meters of UD and BL FLAXPREG (each) were ordered, which is a sufficient amount of material to laminate multiple beams several times. As determined in the calculations from **Appendix A**, attaining an $I_{xx,UD}$ of greater than or equal to 0.658 in^4 is easily achieved by exploiting the allowable 4 inch beam height specified by SAMPE and including 0° UD FLAXPREG as far away from the *x*-axis as possible (in the flanges). The beam dimensions and necessary moments of inertia are very feasible; however – as will be noted in the following section – some of the vacuum bagging and curing methods proved too difficult or ineffective.

The most feasible designs from a manufacturing standpoint have uniform cross sections, as this avoids angled cuts for their poplar plywood cores. It also avoids the requirement of including drafts in any molds used. The wood cores could either be bonded before of after the uncured FLAXPREG was applied. Also, either the epoxy in FLAXPREG or an alternative adhesive could be used to bond the core. Although it was realized early on that the most feasible way to manufacture a beam was to pre-bond the core using a wood glue, enough material was purchased to try alternative bonding methods. One alternative bonding method was attempted for the first beam made.

The dimensional constraints and necessary moments of inertia of each beam were not difficult to satisfy. The primary concern in the feasibility of each design was the manufacturing process. Three beams were manufactured using two manufacturing processes. The dimensions, laminate schedules, and $I_{xx,UD}$ as well as the curing processes used are described in the following section.

V. Preliminary Design

This section will examine the parameters and manufacturing processes of each beams manufactured. It will also present the performance estimates made for the competition beam, and the costs of all materials used.

A. Beam Designs

Three beams were made during the course of this project. In order to increases $I_{xx,UD}$, the 4 inch by 4 inch cross sectional beam height and width allowed by SAMPE, were exploited for each beam. Each beam was given a uniform cross section, as this simplified the cutting of core materials and the vacuum bagging process immensely. In order to minimize weight of the beam, each beam would be made the minimum allowable length of 24 inches. The general beam design for all three beams, as seen in the following section, would consist of two pieces of 3.6 inch by 0.125 inch poplar plywood for the web, one piece of 4 inch by 0.125 inch poplar plywood for each flange, and one 0.375 inch by 0.375 inch concave balsa wood fillet for each corner. Two plies of 45° BL FLAXPREG on each side of the web were included to carry shear. Multiple plies of 0° UD FLAXPREG were included in each flange to carry tension and compression. One ply of 45° BL FLAXPREG was included on the outside of each flange to carry any lateral shear (shear in the *xy*-plane) developed due to unanticipated twisting. For each design, it was ensured that $I_{xx,UD}$ exceeded 0.658 in^4. Since all experience with composite manufacturing was to be gained in the course of this project, changes made to each design were based primarily on the manufacturing success of the previous iteration and not on analysis. All three beams would be manufactured using the vacuum bagging process depicted in **Figures 7** and **8**, which was specifically meant to ensure proper pressure application to the concave balsa wood fillets at the flange-web junctions. Specifications and design changes of all three beams are detailed in the following section.

Design I

A unique feature of the first beam is that its four wood core components were bonded, at the same time as the rest of the beam, using plies of 0° UD FLAXPREG. The laminate schedule for the first beam is shown in **Figure 16**. The UD FLAXPREG included in the second beam had a first moment of area of 0.711 in^4 (**Appendix A**), which exceeds the necessary value of 0.658 in^4 that would prevent failure due to tension. The first moment of area factor of safety ($F.O.S._{tension}$), or $I_{xx,UD}/I_{xx,tens}$, is 1.08 for this design. One of the main problems with the first beam was the way in which the core was bonded. Since the wood core was not already bonded together when the FLAXPREG was being applied, nothing provided the beam with geometric integrity during the curing process. The resulting beam, seen in **Figure 17**, did not maintain the cross-sectional shape of an I-beam, and more closely resembled an italicized 'I'. The non-vertical orientation of the web would

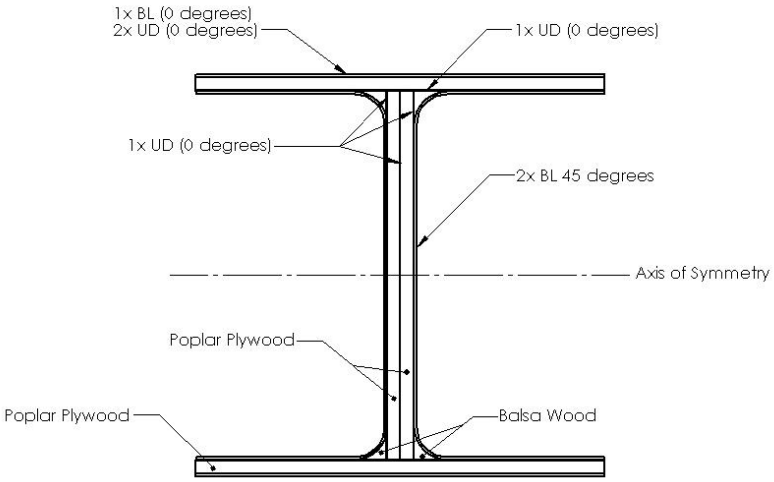

Figure 16. A laminate schedule for I-Beam I is shown.

Figure 17. Two views of the first I-beam are shown. Note the non-vertical orientation of the web.

greatly reduce the shear-carrying capacity of the first beam. If loaded as intended, the flanges and web of the first beam would likely fold in on one another to cause premature failure. Also, the unintended geometry of the first beam resulted in stretching of the FLAXPREG, which consequently bridged the corners between the web and flanges, leaving large pockets of air under layers of the FLAXPREG. These air pockets (that are essentially delaminated zones) could induce further delamination wherever the FLAXPREG managed to bond to the wood, thus causing premature failure. In order to address the shaping problems with the first beam, the manufacturing process of the beam was revisited.

Design II

The major difference between the first and second beam is that the core for the second beam was pre-bonded using Elmer's® Wood Glue Max. As seen in **Figure 18**, this caused the beam to maintain its shape during the laying on of FLAXPREG, thus allowing the laminates to be properly pressed onto the wood core using a plastic tool. This ultimately made the vacuum bagging process easier, and the overall curing process more effective. Although the vacuum bagging process for the second beam was easier than that of the first beam, several problems were still encountered. The uncured FLAXPREG was difficult to adhere to the wood without it sticking to the tools used to remove air pockets from the beneath the laminates. Towards the end of the lamination process it was realized that by leaving on one side of the paper backing, in which the FLAXPREG is shipped, it became

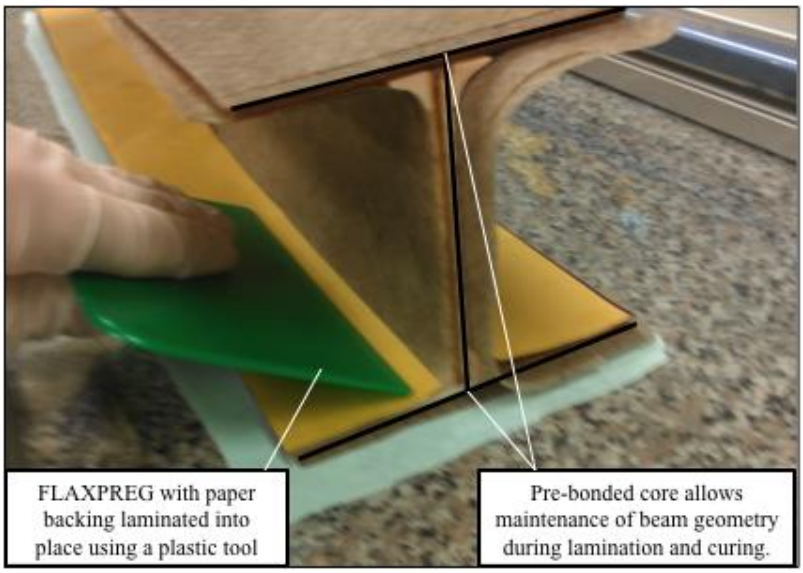

Figure 18. When the beam's core was glued together with Elmer's Wood Glue Max, prior to applying the FLAXPREG, the beam was able to maintain its I-shape.

easier to flatten the fabric onto the wood core (see **Figure 18**). It was also found that when removing the paper backing from the adhered layers of FLAXPREG, the tip of an aluminum rod served as the best tool for keeping the fabric adhered to the wood as opposed to the paper.

Aside from implementation of different manufacturing techniques, the laminate schedule of the second beam was also altered from that of the first. Since the bonding layers of UD FLAXPREG from the first beam design were removed, $I_{xx,UD}$ was greatly reduced. Including two 1.5 inch strips of UD FLAXPREG on each of the inner faces of the flanges made up some of the difference in $I_{xx,UD}$. The laminate schedule for the second beam can be seen in **Figure 19**. The UD FLAXPREG included in the second beam had a first moment of area of 0.720 in^4 (**Appendix A**), which exceeds the necessary value of 0.658 in^4 that would prevent failure due to tension. The $F.O.S._{tension}$ is 1.09 for this design. Although the second beam maintained its geometry and was relatively well bonded, it only had a factor of safety for failure due to tension ($F.O.S._{tension}$) of 1.09 (**Appendix A**). Due to the unpredictability of composite failure, a higher $F.O.S._{tension}$ is desirable. The second beam also contained a few air pockets between the FLAXPREG layers and wood core, which could cause premature failure due to delamination. The low $F.O.S._{tension}$ was addressed by including more UD FLAXPREG in the final lamination schedule. The somewhat delaminated bonding of the second beam was addressed by using only the laminating and vacuum bagging techniques that were observed to work during the manufacturing of the second beam.

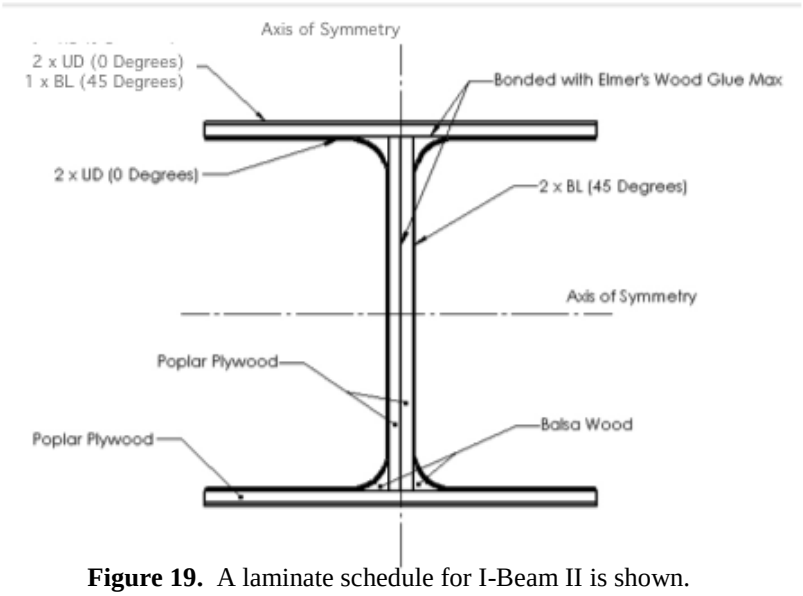

Figure 19. A laminate schedule for I-Beam II is shown.

Design III

The primary difference between the second beam and the third beam was the inclusion of more UD FLAXPREG in the third beam. The lamination schedule of the third beam is shown in **Figure 20**. One extra ply of UD FLAXPREG was included in each of the flanges.

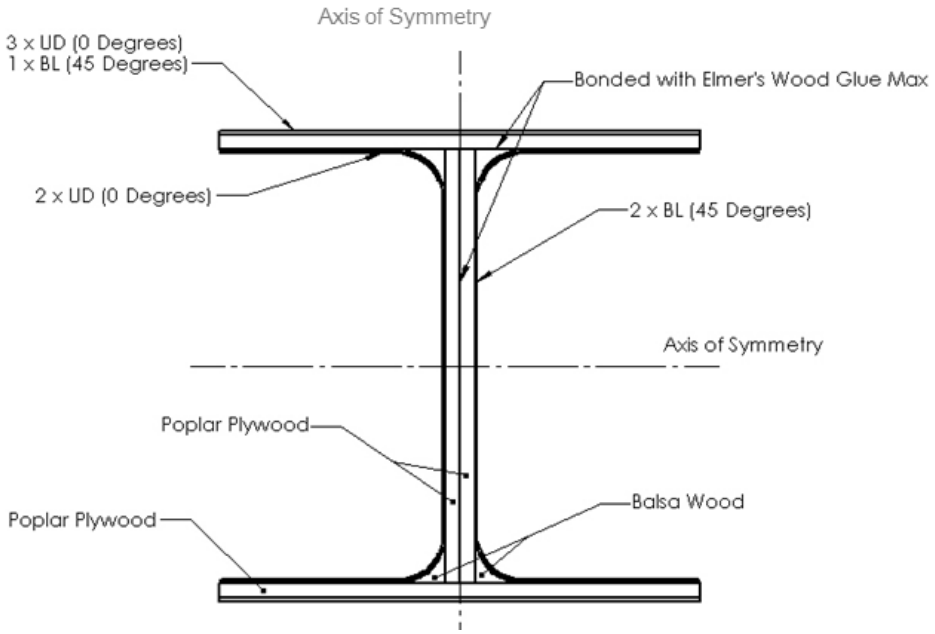

Figure 20. A laminate schedule for I-Beam III is shown.

A schematic of the cross section, highlighting the areas where 0° UD FLAXPREG was included is shown in **Figure 20**. The resulting first moment of area of only the UD FLAXPREG was 0.944 in^4 (**Appendix A**) with a $F.O.S._{tension}$ of 1.43. In order to idealize the bonding of the FLAXPREG to the wood core, lamination methods observed to have worked best for the second beam, were employed immediately during the manufacturing process of the third beam. Such methods included keeping one side of the paper backing on the FLAXPREG when laying down each ply (**Figure 18**), using aluminum rods to hold the FLAXPREG in place

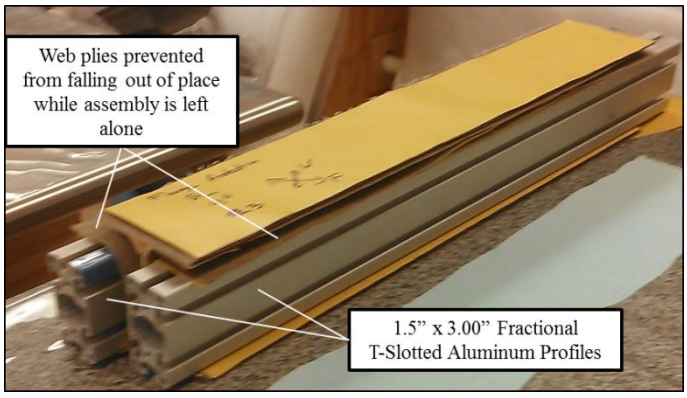

Figure 21. Aluminum profiles held plies of FLAXPREG in place.

while the paper backing was removed, and using 1.5 inch by 3.00 inch fractional T-slotted aluminum profiles to hold the web plies in place (**Figure 21**). Use of the aluminum profiles allowed the assembly to be left in the manufacturing lab over night, during which time the FLAXPREG plies seem to have adhered better to the wood core, thus making the vacuum bagging processes significantly easier. Vacuum bagging was easiest when two sheets of nylon bagging, cut to large dimensions were used as seen in **Figure 22**. Using larger sheets of nylon bagging reduced the number of wrinkles where the bagging was to be sealed, thereby making leaks in the system easier to prevent. By implementing successful lamination methods from the previous two beams and using larger sheets of nylon bagging for the vacuuming process, better vaccuum was achieved in the third beam assembly. As a result, the third and final beam had the least amount of layer seperation.

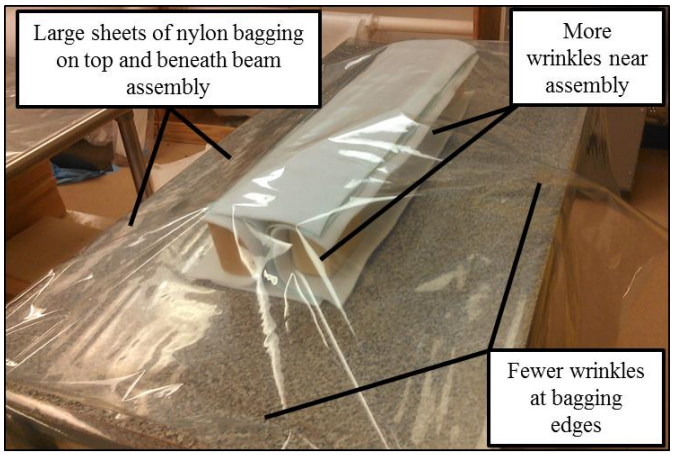

Figure 22. A reduction of wrinkles in the vacuum bagging is achieved by using larger sheets.

D. Performance Estimates and Testing

According to the analysis in **Appendix B**, the maximum bending moment associated with a beam loaded with an arbitrary weight of *P* under competition loading conditions is 5.25*P* in·lbs. Substituting this into **Equation 11** for *M* gives;

$$\sigma_{ult} = \frac{(5.25\text{in})Pc}{I_{xx,UD}} \qquad \textbf{(14)}$$

Isolating *P* and substituting known values into **Equation 14** gives;

$$P = \frac{(47{,}860\text{psi})I_{xx,UD}}{(5.25\text{in})(2\text{in})} \qquad \textbf{(15)}$$

Simplifying gives;

$$P = \left(4{,}558\tfrac{\text{lbs}}{\text{in}^4}\right)I_{xx,UD} \qquad \textbf{(16)}$$

Equation 16 can be used to predict the loads at which beams will fail due to tensile bending normal stress of 0° UD FLAXPREG. For example, Beam I was expected to fail at a load given by;

$$P = \left(4{,}558\frac{\text{lbs}}{\text{in}^4}\right)(0.711\text{in}^4) = 3{,}241\ lbs$$

Similarly, Beams II and III were expected to fail under the same mode at applied loads of 3,282 lbs and 4,303 lbs, respectively. Due to time constraints, no tests were conducted prior to the SAMPE competition in order to validate the performance estimation method used.

E. Cost Analysis

In order to provide incentive for advanced composite users to substitute traditional composite materials with renewable and sustainable natural substitutes, said natural substitutes must be cost effective. The manufacturing process for the natural fiber/natural core I-beams in this project were identical to those of traditional composites, thus the manufacturing materials used were the same. Costs of materials needed to make all three beams and characterization specimen are documented in **Table 2** along with total cost.

Table 2. Items used to make all three beams are documented along with suppliers, quantity used and total cost.

Item	Supplier	Cost/Unit	Qty.	Total Cost
5 yd. BL FLAXPREG 150 g/m^2	LINEO	$213.64	1	$213.64
5 yd. UD FLAXPREG 150 g/m^2	LINEO	$221.34	1	$221.34
5 yd. Nylon Release Peel Ply	Fibre Glast Development Corp.	$49.95	1	$49.95
7 oz. 5 yd. Breather and Bleeder	Fibre Glast Development Corp.	$39.95	1	$39.95
5 yd. 60"/120" Wide Centerfold Stretchlon 200 Bagging Film	Fibre Glast Development Corp.	$39.95	1	$39.95
Gray Sealant Tape	Fibre Glast Development Corp.	$7.95	2	$15.90
Vacuum Connector	Fibre Glast Development Corp.	$4.95	2	$9.90
0.5 hp Pumps Electric Power	NA	NA	NA	NA
Autoclave Electric Power	NA	NA	NA	NA
Autoclave Water Supply	NA	NA	NA	NA
		Total Cost		$590.63

To purchase a 50 inch wide, 5 yard roll of carbon fiber pre-preg would cost $654.45 and to purchase 50 inch wide, 5 yard roll of fiberglass pre-preg would cost $241.95.[20] This puts carbon fiber pre-preg and fiberglass pre-preg at $10.47/ft^2 and $3.87/ft^2, respectively. BL FLAXPREG is $3.97/ft^2 and UD FLAXPREG is $4.11/ft^2. Both types

of FLAXPREG are remarkably cheaper than carbon fiber pre-preg; however, each is slightly more expensive than fiberglass, suggesting that there is no cost incentive to use flax fibers over fiberglass yet. This may change as less expensive fiber treatments are developed to prevent dewetting. In spite of the lack of fiscal incentive to use flax fiber over fiberglass at the moment, flax fibers still act as light-weight, effective composite reinforcements. The following section reveals as much by examining the results of the SAMPE competition.

VI. Results and Recommendations

This section will discuss the performance of the competition beam at the SAMPE Student Bridge Contest. It will examine how the beam failed, and speculate as to why failure occurred. It will then make recommendations for next year's competition, concerning the characterization of materials, beam optimization, and simplified manufacturing processes.

A. Results

The final beam manufactured for this project was to withstand 3,000 lbs under competition loading conditions while maintaining a low weight. In order to ensure that the beam did not catastrophically fail or deflect an inch or greater prior to being loaded with 3,000 lbs, the necessary first moment of area of exclusively 0˚ UD FLAXPREG in the beam was calculated, and found to be 0.658 in^4. The final beam design's value of $I_{xx,UD}$ was 0.944 in^4, giving it a factor of safety of 1.43 with regards to tensile failure. The beam was manufactured by pre-bonding four wood core pieces using Elmer's WoodGlue Max, then laminating the core with plies of BL FLAXPREG and UD FLAXPREG. The assembly was then vacuum bagged, and put into Union College's Manufacturing Facility's autoclave at 230 °F and 2 atm for 2 hours. The final beam was relatively well bonded with few areas layer separation. The final beam's maximum cross sectional dimensions were roughly 4 inches by 4 inches, and its length was roughly 24 inch.

At the competition, the beam was passed through square plastic ring with a 4 inch by 4 inch hole in it. Since the beam was designed with a 4 inch by 4 inch cross section with loose tolerances, it ended up being larger than 4 inches by 4 inches. Understandably, it was difficult to pass the beam through aforementioned plastic ring and its flanges had to be trimmed on sight. Future beam designs should have tighter upper dimensional tolerance limits of 4 inches or less. Once the beam was forced through the hole it was further inspected by the competition committee and weighed. The beam was the lightest in the natural fiber I-beam category with a mass of 610.7 g. The beam was loaded with up to 2,090 lbs, after which point the web twisted and caused the top flange to move independently of the bottom flange until it deflected 1 inch. Ultimately, the beam had a strength-to-weight ratio of 1,550 if loaded as intended. This indicates that

natural fiber reinforcements and natural cores may be used to fabricate high-performance composites. However, the beam did not manage to carry the intended load of 3,000 lbs, and did poorly in the SAMPE Student Bridge Contest as a result. Furthermore, the beam did not include a naturally derived thermoset as its resin matrix and the beam was not completely sustainable from a materials standpoint. Several steps may be taken in order to address these problems.

The beam in the competition failed prematurely, suggesting that not all failure modes were properly considered during analysis. Incomplete analysis is partly due to the lack of material properties provided by LINEO for UD FLAXPREG and BL FLAXPREG. Any materials used for future competition entries by Union College should be properly characterized in Union College's testing facilities. This may be achieved by hot-pressing 4 to 8 plies of the materials to be used, according to manufacturer-specified curing cycles. Different laminate schedules should be cured for testing. For example, in order to characterize UD and BL FLAXPREG, laminate schedules such as the following should be hot-pressed;

- UD <0°, 90°, 0°, 90°>
- UD <0°, 90°, 90°, 0°>
- BL <0°, 45°, 45°, 0°>

During this process, consult Professor R. Bucinell about how to maintain symmetry between the plies to avoid warping. The hot-pressed samples should then be cut into tensile specimen, their cross-sectional dimensions should be measured, and they should be loaded under tension until failure occurs. Proper analysis of repeated tensile tests should provide needed mechanical properties along primary axes to allow for proper failure analysis, including finite element analysis in SolidWorks and SimulationXpress. Whether or not characterization of materials used in the future is conducted, the failure mode incurred on 2013's beam design should be examined.

As seen in **Figure 23**, failure of the beam was caused by 1 inch deflection of the top flange. Said deflection occurred because, after a 2,090 lb load was applied, the web began to twist. The cause of this twisting was not identified until after the beam was removed from the loading apparatus and examined. As seen in **Figure 24**, the bottom flange developed a large crack directly beneath the web. This was presumably due to a stress concentration at the junction of the web and flange which induced large shear stresses and tore the bottom flange.

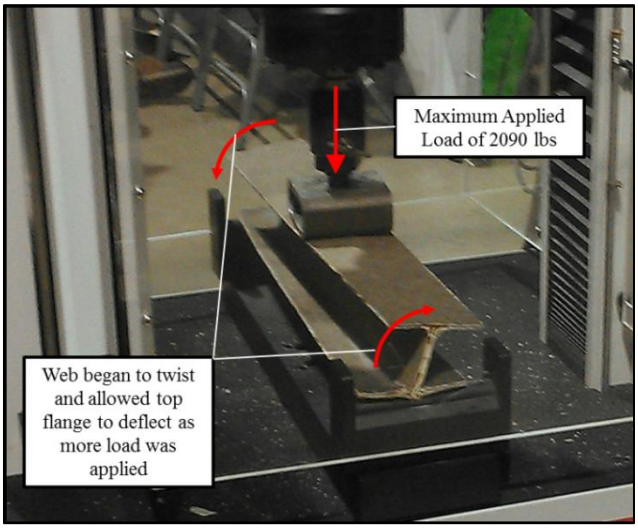

Figure 23. The beam is shown in the competition loading apparatus. Once the applied load reached 2,090 lbs, the beam simply began to deflect and yield to further loading.

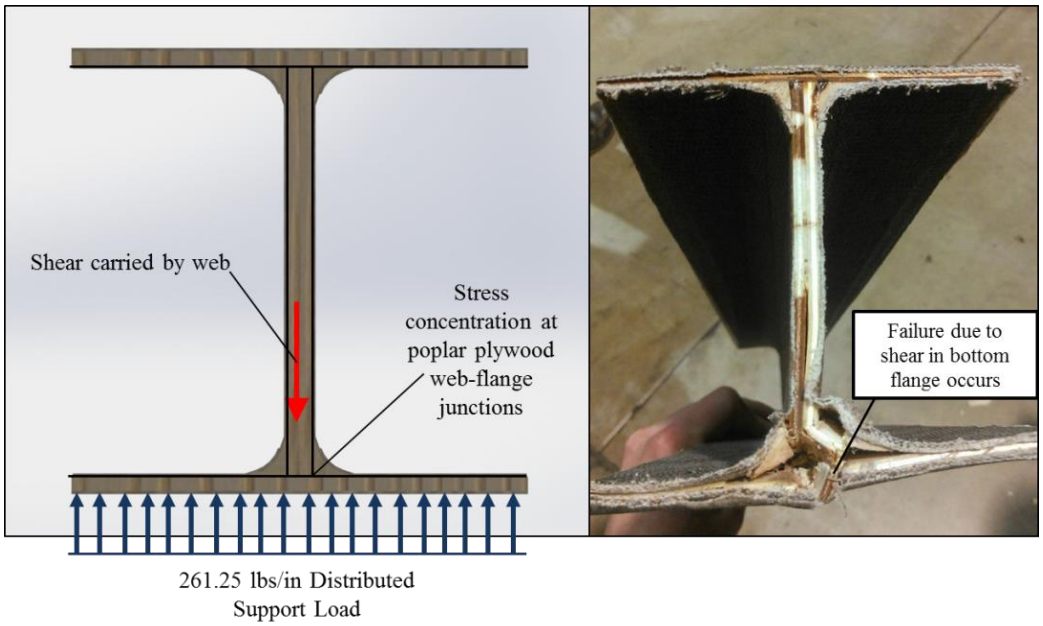

Figure 24. Left: An annotated schematic of the beam cross section depicts where a large stress concentration occurred and induced large shear forces. **Right:** A picture of the actual beam once removed from the loading apparatus shows where resulting failure occurred.

The laminate schedule of the bottom flange only consisted of three plies of 0° UD FLAXPREG buffered with one ply of 45° BL FLAXPREG. UD FLAXPREG plies will not effectively stop crack propagation along their weft directions (the *z*-axis in this case)

and one ply of 45° BL FLAXPREG is not enough to stop crack propagation for substantial shear loads. As a result, the crack that started in the bottom flange at one of the supports propagated towards the center of the beam. As the crack extended and the bottom flange was allowed to separate, it lost its ability to carry unexpected shear in the *xy*-plane due to twisting. Once this occurred, twisting of the web – an indicator of torsion and non-centric loading – was observed, probably due to imbalanced loading. The loading may not have been balanced because the beam was put into the loading apparatus by hand. As seen in **Figure 25**, said torsion applied tension to the 45° BL FLAXPREG on one side of the web and compression to the 45° BL FLAXPREG on the other side.

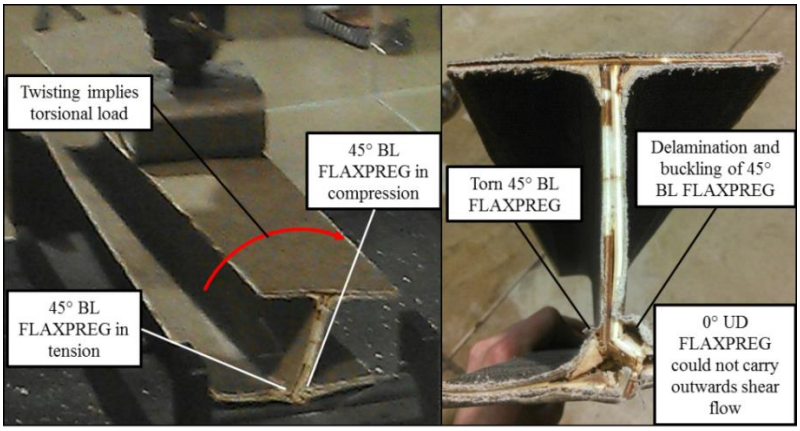

Figure 25. Left: The twisting beam in the loading apparatus is shown, with the areas where tension and compression develop clearly labeled. **Right:** A cross sectional view of the beam shows how ineffectively 45° BL FLAXPREG was able to carry tension and compression.

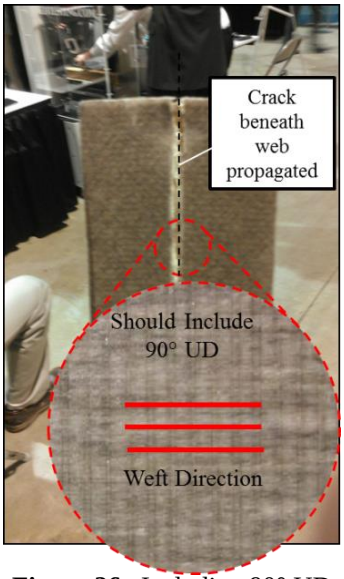

Figure 26. Including 90° UD FLAXPREG in the bottom flange would help prevent crack propagation.

In order to prevent *z*-direction crack propagation in the bottom flange, more plies of 45° BL FLAXPREG should be included to carry shear in the *xy*-plane, and one or two plies of 90° UD FLAXPREG should be included to interrupt propagation. The way in which 90° UD FLAXPREG should be incorporated into the flange is denoted in **Figure 26**. In order to prevent (or at least diminish) torsion, subsequent twisting, and subsequent deflection in future competitions the beam should be placed as close to a centered position in the apparatus as possible. It may be beneficial to ask the judges if the loading block can be lowered until directly in contact with the beam, but such that no load is applied. This

way, more care can be taken to position the beam. Although prevention of mechanical failure will likely result in a more competitive design for Union College in future SAMPE competitions, it will not address the primary focus of working with sustainable materials.

Focus for future work by Union College should be on fabricating composites made from entirely renewable resources. It has already been demonstrated that natural fiber reinforcements and natural core materials are suitable for high-performance applications. In fact, flax fibers remain the recommended natural fiber reinforcement. Exploration of alternative core materials, such as any of the mycelium products developed by Ecovative, may prove beneficial; however, immediate focus for next year's SAMPE student bridge contest should be on using a naturally derived thermoset resins for bonding the natural fibers to the natural cores. One such option is to explore using linseed oil-based polymer thermosets being developed at Rensselaer Polytechnic Institute. Using an externally applied thermoset resin, as opposed to a pre-preg (as was done for 2013's design), will likely alter the manufacturing process, but it will present the option of competing in the natural fiber square beam category, which prohibits use of pre-pregs. Although experience from this project was gained using only pre-pregs, several composite manufacturing recommendations may be made based on said experience and observations from the 2013 SAMPE convention.

B. Recommendations

Regardless of the materials used for future competitions, the first recommended step is still to cure samples of the material and characterize their mechanical properties. It should also be noted whether or not the resin properly bonds to the fibers used, or if treatment of the fibers will be necessary to prevent dewetting. This should be done well in advanced of the competition so that any delayed degradation of the cured materials may be noted. Several beam designs should be modeled in SolidWorks and SimulationXpress using anisotropic material properties based on the characterization conducted. (See ***SolidWorks Help***, ***Simulation***, ***Composite Shells*** or for a tutorial, go to ***Office Product***, ***SolidWorks Simulation***, and pull down ***Help***, ***SolidWorks Simulation***, ***Simulation Tutorials***, ***Static***, ***Composite Shells***.) The models should each heed the post-

competition recommendations made about including more plies of 45° BL FLAXPREG and 90° UD FLAXPREG in the bottom flange. If time permits, the beams should be optimized for weight such that it will still withstand competition loading conditions bearing in mind that complicating the geometry of the beam may complicate the manufacturing process. One easy way to do this is to vary the width of the flanges by trimming them after the beam is cured. The flanges may be trimmed according to the following equations derived in **Appendix B**;

$$w_{[0\le z\le 9.5]} = \frac{2(0.5Pz)}{\sigma_{all}\left[\frac{1}{6}t^3+2t(c-0.5t)^2\right]} \quad \textbf{(17)}$$

$$w_{[9.5<z\le 13.5]} = \frac{2\left(-0.125Pz^2+2.875Pz-11.281P\right)}{\sigma_{all}\left[\frac{1}{6}t^3+2t(c-0.5t)^2\right]} \quad \textbf{(18)}$$

$$w_{[13.5<z\le 23]} = \frac{2(-0.5Pz+11.5P\ )}{\sigma_{all}\left[\frac{1}{6}t^3+2t(c-0.5t)^2\right]} \quad \textbf{(19)}$$

Where P is the applied load, z is the horizontal position along the length of the beam, σ_{all} is the allowable tensile stress associated with whatever 0° UD material is used, t is flange thickness (if constant with respect to z) and c is half of the beam's height (if constant with respect to z).

The manufacturing process for a non-pre-preg based composite is largely similar to that of a pre-preg based composite. Vacuum bagging the beam in the Union College Manufacturing Lab's autoclave is still likely the best manufacturing process to use. In this project, vacuum bagging was conducted such that the bagging followed the contours of every surface on the I-beam as seen in **Figure 8**. However, the process may be simplified by using aluminum tooling or extrusions as seen in **Figure 27**. By laying down the peel ply and breather/bleeder layers, then placing aluminum molds between the flanges, the vacuum bagging assembly would maintain geometric integrity on its own. Wrapping the entire assembly shown in **Figure 27** in vacuum bagging, then evacuating the air would achieve almost the same curing

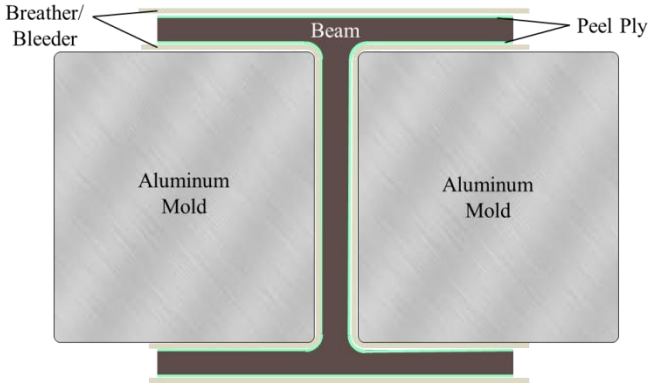

Figure 27. A cross sectional view of an alternative vacuum bagging method is shown.

quality while greatly increasing manufacturability. It should be noted that if this approach is taken, geometric tolerances of the beam in between the web become crucial, as the molds cannot apply pressure to the flanges unless they fit relatively snuggly, in which case they will apply pressure due to thermal expansion. The high thermal conductivity of aluminum would ensure that relatively even heat distribution to the web is still achieved in the autoclave.

The following section will restate the goals of this project, the results of the steps taken to achieve said goals, and reemphasize the recommendations made in this section.

VII. Conclusion

The goal of this project was to demonstrate the applicability of natural fiber reinforcements and core materials in high-performance composites by competing in the 16th Annual SAMPE Student Bridge Contest with flax fiber-reinforced, wood-core composite I-beam. By using naturally derived and therefore renewable materials in composites, a great deal of non-renewable resources such as fossil fuels could be saved for alternative uses. Secondary goals of this project were to familiarize Union College's Mechanical Engineering Department's students with advanced composite manufacturing. While the final beam manufactured for competition held 2,090 lbs and only weighed 1.35 lbs, it could not withstand the intended load of 3,000 lbs. That being said, it has become fully apparent that natural fiber reinforcements and natural core materials are suitable for use in some high-strength, low-weight composite designs. A great deal of information was learned during the course of this project that could further Union College's involvement with natural composites. In order to further demonstrate the applicability of natural materials in advanced composites, improvements to the design process, design, material composition and manufacturing process can be made for beams entered into future SAMPE competitions, including;

- Mechanical characterization of the materials used in the beam;
- Modeling of the beam designs in SolidWorks and finite element analysis in SimulationXpress based on the characterized properties;
- Inclusion of 90° UD plies and more 45° BL plies of natural fiber fabric in the bottom flange;
- Geometric optimization of one or more of the beam dimensions to increase the strength-to-weight ratio of the beam based on a selected failure mode;
- Exploration of alternative natural core materials;
- Use of a naturally derived thermoset resin to bond the fibers to the core;
- And use of tooling aluminum as molds to hold the beam together during vacuum bagging and curing.

If the recommendations in this report are heeded, a great deal of improvement can be made regarding Union College's performance in the 2013 SAMPE Student Bridge Contest, and awareness can be spread regarding the availability of natural materials as traditional composite material substitutes.

References

1. "Composite." Merriam-Webster®. *Web*. February 1, 2013. <www.merriam-webster.com>
2. Johnson, Todd. "Applications of Carbon Fiber: What Products Use Carbon Fiber Today." *Web*. May 14, 2013. <composite.about.com>
3. Gardiner, Ginger. "The making of glass fiber." COMPOSITES WORLD. *Web*. May 14, 2013. <www.compositesworld.com>
4. "Reinforcements." ROM Development Corporation: Core Composites. *Web*. May 14, 2013. <www.corecomposites.com>
5. "Aramid." CIRFS: European Man-made Fibres Association. *Web*. May 14, 2013. <www.cirfs.org>
6. McConnell, Vicki. "The making of carbon fiber." COMPOSITES WORLD. *Web*. May 14, 2013. <www.compositesworld.com>
7. "Polystyrene Foam Report." EARTH RESOURCE FOUNDATION. *Web*. May 14, 2013. <www.earthresource.org>
8. "Epoxy 101: What is Epoxy?" Construction Systems Supply. *Web*. May 14, 2013. <www.csscorp.net>
9. "Environmental Concerns." WEST SYSTEM®. *Web*. May 14, 2013. <www.westsytem.com>
10. Johnson, Todd. "Recycling Composite Materials: End Of Life Solution for FRP Composites." *Web*. May 15, 2013. <composite.about.com>
11. ecovative. Ecovative Deign LLC. *Web*. May 14, 2013. <www.ecovativedesign.com>
12. Waifielate, A. and Abiola, Bolarinwa O. "Mechanical Property Evaluation of Coconut Fibre." Department of Mechanical Engineering Blekinge Institute of Technology. Karlskrona, Sweden 2008. *Web*. January 21, 2013. <http://www.bth.se/>
13. Luo, S. and Netravali, A. "Polymer Composites: Mechanical and thermal properties of environment-friendly "green" composites made from pineapple leaf fibers and poly(hydroxybutyrat-co-valerate) resin." Volume 20, Issue 3. Abstract. April 15, 2004. *Web*. January 21, 2013. <onlinelibrary.wiley.com>
14. Hu, R. and Lim, J. "Journal of Composite Materials: Fabrication and Mechanical Properties of Completely Biodegradable Hemp Fiber Reinforced Polylactic Acid Comosites." Volume 41, Issue 13. Abstract. July 2007. *Web*. January 21, 2013 <jcm.sagepub.com>

15. Shahazad, A.; Isaac, D. and Alston, S. "Mechanical Properties of Hemp Fiber Composites." Materials Research Center, Swansea University, Singleton Park, Swansea, UK. *Web*. January 21, 2013. <www.google.com>

16. Spārņiš, E. "Mechanical properties of flax fibers and their composites." Department of Applied Physics and Mechanical Engineering, Luleå University of Technology. *Web*. January 23, 2013. <epubl.ltu.se>

17. Oohi, S. "Tensile Properties of Bamboo Fiber Reinforced Biodegradable Plastics." Department of Mechanical Engineering, Niihama National College of Technology, Niihama City, Japan. *Web*. January 23, 2013. <google.com>

18. "E-Glass Fibre." AZoM. *Web*. June 7, 2013. <www.azom.com/articl.aspx?ArticlID=764>

19. "KEVLAR®: Aramid Fiber: Technical Guide." *Web*. June 7, 2013. <www2.dupont.com/Kevlar/en_US/assets/downloads?KEVLAR_Technical_Guid.pdf>

20. "Technical." DragonPlate™. *Web*. June 7, 2013. <dragonplate.com/section/technology.asp>

21. *Mechanical Design in Optical Engineering: Sheer Stresses in Beam*s. The University of Arizona®. *Web*. June 8, 2013. <http://fp.optics.arizona.edu>

22. "FLAX FIBER IMPREGNATION: Powerful by nature…" LINEO$_{NV}$. *Web*. April 10, 2013. <www.lieo.eu>

23. Ruina, Andy. "BEAM DEFLECTION FORMULAE." *Web*. February 4, 2103. <ruina.tam.cornell.edu>

24. Fibre Glast Developments Corporation. *Web*. May 27, 2013. <www.fibreglast.com>

25. Avérous, Luc and Pollet, Eric. "Environmental Silicate Nano-Biocomposites: Biodegradable Polymers." Springer 2012, Vermont.

26. Westman, M. P.; Fifield, L. S.; Simmons, K. L.; Laddha, S. G. and T. A. Kafentzis. "Natural Fiber Composites: A Review." Pacific Northwest National Laboratory. March 2010.

27. Bledzki, A. K.[1]; Mamun, A. A.[1]; Lucka-Gabor, M.[1] and V. S. Gutowski[2]. "The effects of acetylation on properties of flax fibre and its polypropylene composites." [1]Institut für Werkstofftechnik, Kunststoff- und Recyclingtechnik University of Kassel. Kassel, Germany. [2]CSIRO Manufacturing & Infrastructure Technology, Novel Materials & Processes. Melbourne, Australia. April 2008.

28. Tsai, S. W.[1] and E. M. Wu.[2] "A General Theory of Strength for Anisotropic Materials." [1]Air Force Materials Laboratory. [2]Washington University. St. Louis, MO. August 1972.

Appendix A: Calculation of $I_{xx,UD}$

The thickness of UD FLAXPREG was measured with calipers at various locations and averaged. It was found that a single ply of UD FLAXPREG is roughly 0.009" thick. In order to remain conservative in the calculation of first moments of area, and account for probable decrease in prepreg thickness after curing, the thickness used was presumed to be 25 % lower, around 0.007".

In order to calculate $I_{xx,UD}$, the cross sections of all 0˚ UD FLAXPREG were treated as rectangles and parallel axis theorem was used. Parallel axis theorem states;

$$I_{xx,tot} = \sum_{i=1}^{n}\left(I_{xx,i} + A_i {d_i}^2\right) \qquad \textbf{(20)}$$

Where $I_{xx,tot}$ represents the first moment of area of the body, $I_{xx,i}$ represents the first moment of area of each section about their centroidal x-axes (axes parallel to the x-axis), A_i represents the cross sectional area of each section, d_i represents the distance from the x-axis to the centroidal x-axis of each section, and i simply denotes each section. For rectangular cross sections, $I_{xx,i}$ is given by;

$$I_{xx,i} = \frac{1}{12} b_i {h_i}^3 \qquad \textbf{(21)}$$

Where b_i is the width of each cross section (x dimension), and h_i is the height of each cross section (y dimension). Also, A_i is given by;

$$A_i = b_i h_i \qquad \textbf{(22)}$$

Substituting **Equation 21** and **Equation 22** into **Equation 20** gives;

$$I_{xx,tot} = \sum_{i=1}^{n}\left[\left(\tfrac{1}{12} b_i {h_i}^3\right) + b_i h_i {d_i}^2\right] \qquad \textbf{(23)}$$

Equation 23 was used to calculate $I_{xx,UD}$ for all three beams in the following sections.

Appendix A: Calculation of $I_{xx,UD}$

Beam I with Sample Calculations

The areas in which UD FLAXPREG was included in Beam I are highlighted in **Figure 28**.

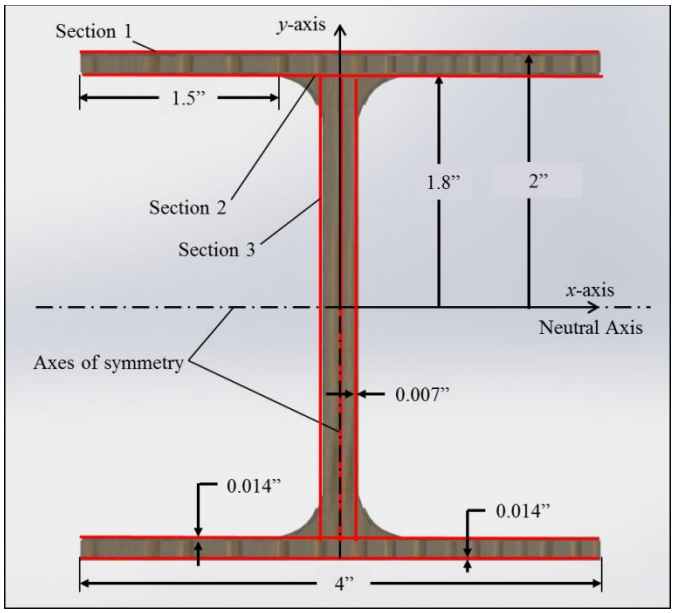

Figure 28. A cross-sectional view of Beam I highlights the areas containing 0˚ UD FLAXPREG and denotes their typical dimensions.

Three UD FLAXPREG sections are shown in **Figure 28**. There are 2 occurrences of Section 1 (Qty._1), two occurrences of Section 2 (Qty._2), and three occurrences of Section 3 (Qty._3). Taking these quantities into account, **Equation 23** can be written as**;**

$$I_{xx,UD} = \text{Qty.}_1\left[\left(\tfrac{1}{12}b_1h_1{}^3\right) + b_1h_1d_1{}^2\right] + \text{Qty.}_2\left[\left(\tfrac{1}{12}b_2h_2{}^3\right) + b_2h_2d_2{}^2\right] + \text{Qty.}_3\left[\left(\tfrac{1}{12}b_3h_3{}^3\right) + b_3h_3d_3{}^2\right] \quad \textbf{(24)}$$

Where the subscripts 1, 2, and 3 represent Section 1, Section 2 and Section 3, respectively. Substituting known values into **Equation 24** gives;

$$I_{xx,UD} = 2\left[\left(\frac{1}{12}\cdot 4\cdot 0.014^3\right) + 4\cdot 0.014\cdot 2^2\right] + 2\left[\left(\frac{1}{12}\cdot 4\cdot 0.007^3\right) + 4\cdot 0.007\cdot 1.8^2\right] + 3\left[\left(\frac{1}{12}\cdot 0.007\cdot 3.6^3\right) + 0.007\cdot 3.6\cdot 0^2\right]$$

Therefore;

$$I_{xx,UD} = 0.711 \text{ in}^4$$

Appendix A: Calculation of $I_{xx,UD}$

Table 3 provides b_i, h_i, A_i, d_i, and Qty. for each section of Beam I. These numbers were used to calculate $I_{xx,UD}$ in Excel.

Table 3. All values needed to calculate $I_{xx,UD}$ and $I_{xx,UD}$ itself are recorded for Beam I.

Section	b (in)	h (in)	A (in^2)	d (in)	Qty.	Qty.×(1/12)bh^3 (in^4)	Qty.×Ad^2 (in^4)
1	4	0.014	0.056	2	2	1.83E-06	0.448
2	4	0.007	0.028	1.8	2	2.29E-07	0.181
3	0.007	3.6	0.0252	0	3	0.082	0.000
					Sums	0.082	0.629
					$I_{xx,UD}$ (in^4)	**0.711**	

Beam II

The areas in which UD FLAXPREG was included in Beam II are highlighted in **Figure 29**.

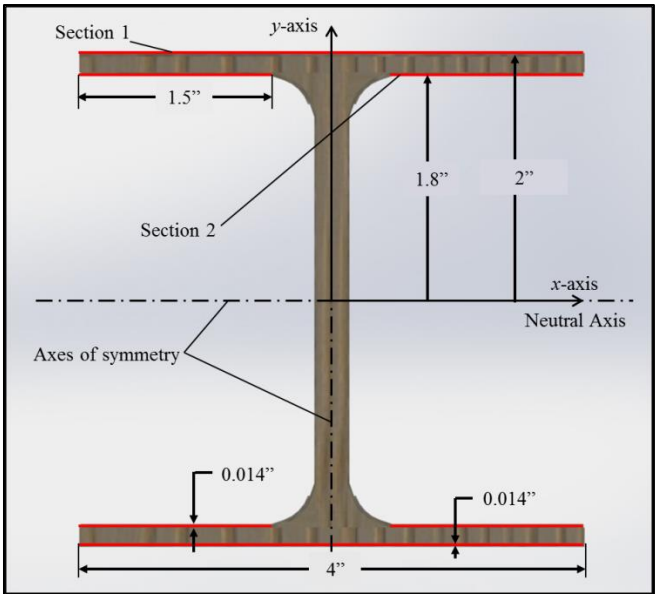

Figure 29. A cross-sectional view of Beam II highlights the areas containing 0˚ UD FLAXPREG and denotes their typical dimensions.

Table 4 provides b_i, h_i, A_i, d_i, and Qty. for each section of Beam II. These numbers were used to calculate $I_{xx,UD}$ in Excel.

Table 4. All values needed to calculate $I_{xx,UD}$ and $I_{xx,UD}$ itself are recorded for Beam II.

Section	b (in)	h (in)	A (in^2)	d (in)	Qty.	Qty.×(1/12)bh^3 (in^4)	Qty.×Ad^2 (in^4)
1	4	0.014	0.056	2	2	1.83E-06	0.448
2	1.5	0.014	0.021	1.8	4	1.37E-06	0.272
					Sums	3.20E-06	0.720
					$I_{xx,UD}$ (in^4)	**0.720**	

Appendix A: Calculation of $I_{xx,UD}$

The areas in which UD FLAXPREG was included in Beam III are highlighted in **Figure 30**.

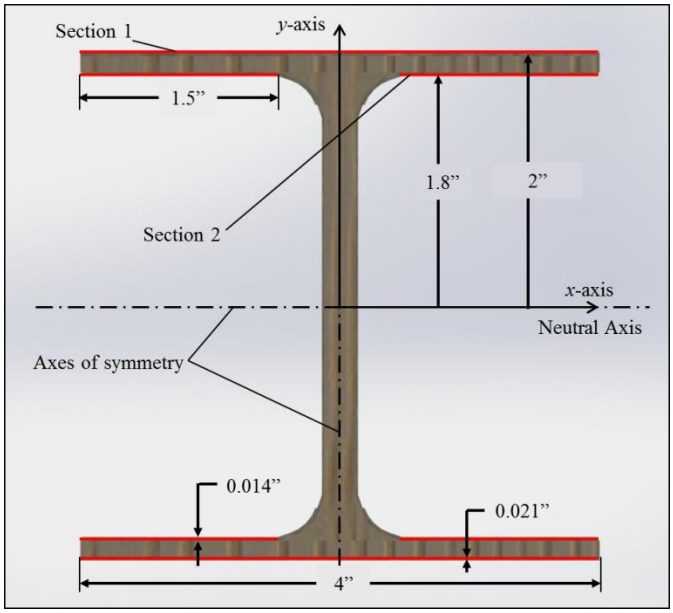

Figure 30. A cross-sectional view of Beam II highlights the areas containing 0˚ UD FLAXPREG and denotes their typical dimensions.

Table 5 provides b_i, h_i, A_i, d_i, and Qty. for each section of Beam III. These numbers were used to calculate $I_{xx,UD}$ in Excel.

Table 5. All values needed to calculate $I_{xx,UD}$ and $I_{xx,UD}$ itself are recorded for Beam III.

Section	b (in)	h (in)	A (in^2)	d (in)	Qty.	Qty.×(1/12)bh^3 (in^4)	Qty.×Ad^2 (in^4)
1	4	0.021	0.084	2	2	6.17E-06	0.672
2	1.5	0.014	0.021	1.8	4	1.37E-06	0.272
					Sums	7.55E-06	0.944
					$I_{xx,UD}$ (in^4)	**0.944**	

Appendix B: Flange Width

This analysis provides the necessary flange width as a function of the ultimate tensile strength (σ_{all}) of characterized 0° UD material, the thickness of 0° UD material used in the beam design, position along the *z*-axis, and the applied load (*P*). Assume competition loading dimensions. Also assume that the beam is 4" high. Consider a generic loading scenario with competition dimensions and an arbitrary applied load (**Figure 31**). Conduct similar analysis to that in the **Background** section, while referencing **Figure 32**.

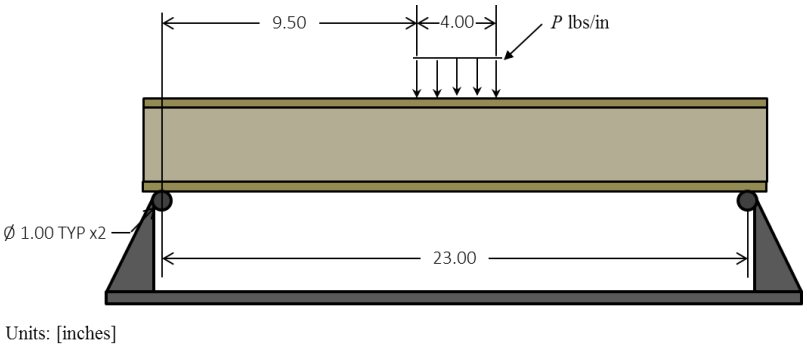

Figure 31. An arbitrarily loaded beam of specified competition dimensions is shown.

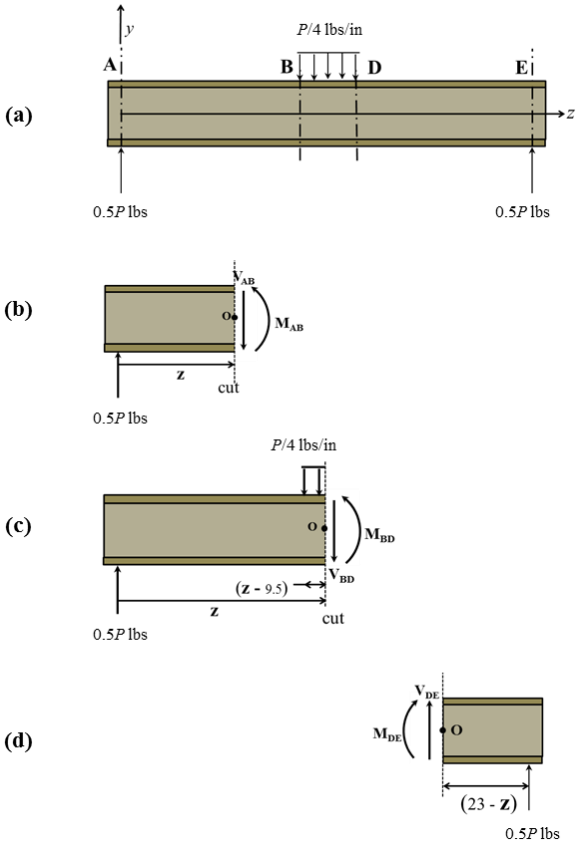

Figure 12. **(a)** A free body diagram of the beam is shown with labeled axes. **(b)** A cut was made between **A** and **B** and a free body diagram of the beam to the left of the cut is shown. **(c)** A cut was made between **B** and **D** and a free body diagram of the beam to the left of the cut is shown. **(d)** A cut was made between **D** and **E** and a free body diagram of the beam to the right of the cut is shown.

Appendix B: Flange Width

Recall that since the beam is in static equilibrium, the sum of all forces and the sum of all moments about some point, *O*, are both equal to zero;

$$\sum F = 0 \qquad \textbf{(1)}$$

$$\sum M_o = 0 \qquad \textbf{(2)}$$

Use of **Equation 1** and **2** allows *V* and *M* to be found as functions of the longitudinal distance away from the left support in **Figure 32(a)** (*z*). For example, **Equation 1** for section BD of the beam is as follows;

$$+\uparrow \sum F_y = 0 = 0.5P - P(z - 9.5) - V_{BD} \text{ [lbs]}$$

Solving for $\boldsymbol{V_{AB}}$ gives;

$$V_{BD} = 2.875P - 0.25Pz \text{ [lbs]}$$

Equation 2 for section BD of the beam about point *O* is as follows;

$$+\circlearrowleft \sum M_o = 0 = -.5Pz + \left(\frac{z-9.5}{2}\right)\left[\frac{p}{4}(z - 9.5)\right] + M_{BD} \text{ [in*lbs]}$$

Solving for M_{BD} gives;

$$M_{BD} = -Pz^2 + 1.875Pz - 11.281P \text{ [in*lbs]}$$

Such analysis provides the following equations for *V* and *M* in the three beam sections;

$$V_{AB} = 0.5P \text{ [lbs]} \qquad \textbf{(3)}$$

$$V_{BD} = -0.25Pz + 2.875P \text{ [lbs]} \qquad \textbf{(4)}$$

$$V_{DE} = -0.5P \text{ [lbs]} \qquad \textbf{(5)}$$

$$M_{AB} = 0.5Pz \text{ [in·lbs]} \qquad \textbf{(6)}$$

$$M_{BD} = -0.125Pz^2 + 2.875Pz - 11.281P \text{ [in·lbs]} \qquad \textbf{(7)}$$

$$M_{DE} = -0.5Pz + 11.5P \text{ [in·lbs]} \qquad \textbf{(8)}$$

Appendix B: Flange Width

Equations 3 through **5** and **Equations 6** through **8** are plotted in **Figure 33** from $0 \leq z \leq 23$ inches.

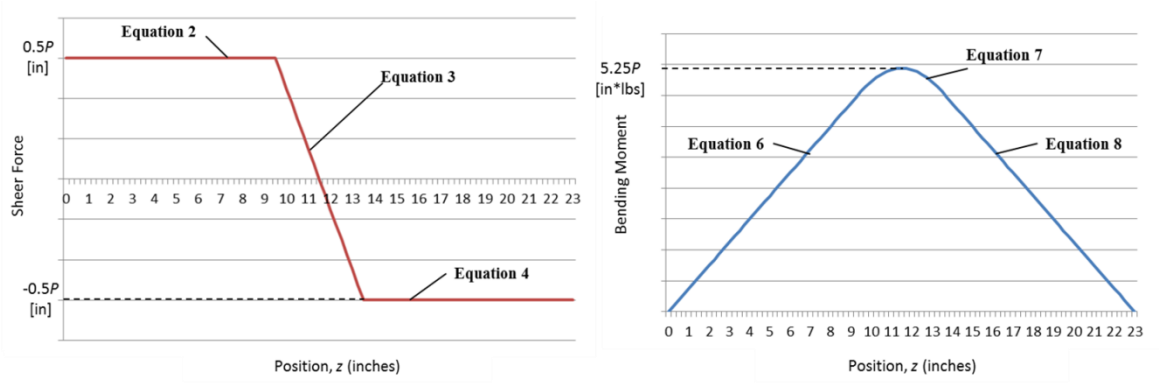

Figure 33. Left: Shear force is plotted with respect to position. **Right:** Bending moment is plotted with respect to position.

Recall that bending normal stress in a simply supported, centrally loaded beam is given by;

$$\sigma_z = \frac{My}{I_{xx}} \qquad \textbf{(9)}$$

Where, in this case, M is the internally developed bending moment, y is the distance from the neutral axis, and I_{xx} is the first moment of area of the cross section of only 0° UD material. M can be taken as **Equations 6**, **7** and **8** for the ranges $[0 \leq z \leq 9.5]$ inches, $[9.5 < z \leq 13.5]$ inches, and $[13.5 < z \leq 23]$ inches, respectively. Failure of material due to bending normal stresses will likely occur at a maximum distance from the neutral axis (c) for which the allowable maximum value is 2" according to competition rules. Suppose that the 0° UD material in the beam

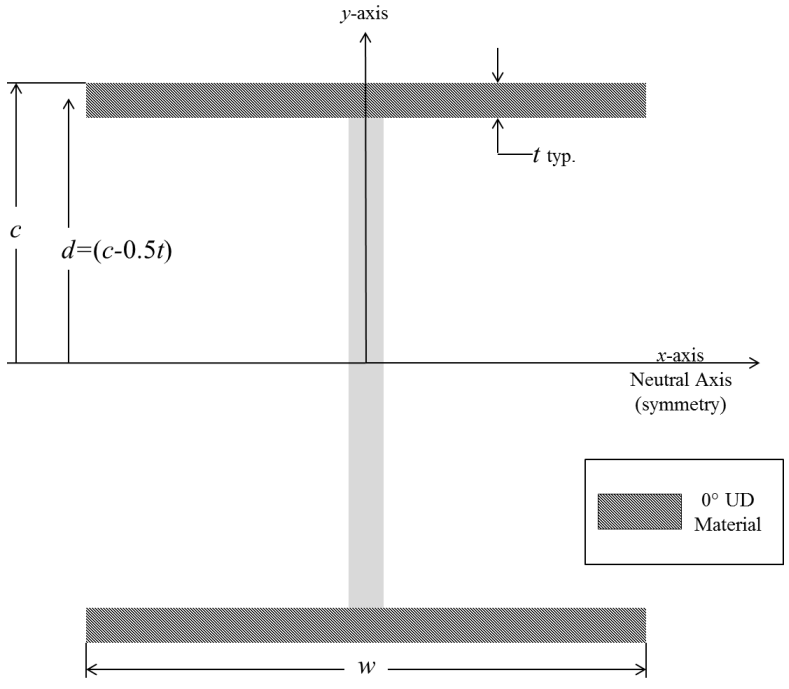

Figure 34. A schematic of the cross sectional area of an I-beam highlights where 0° UD fibers might be incorporated.

Appendix B: Flange Width

is incorporated as highlighted in **Figure 34**. According to parallel axis theorem (see **Equation 20**) the first moment of area becomes;

$$I_{xx} = 2\left[\frac{1}{12}wt^3 + wt(c-0.5t)^2\right] \quad \textbf{(24)}$$

Factoring out *w* and distributing the coefficient of 2 in **Equation 24** gives;

$$I_{xx} = w\left[\frac{1}{6}t^3 + 2t(c-0.5t)^2\right] \quad \textbf{(25)}$$

Substituting **Equations 6**, **7**, and **8** for *M* in **Equation 9** for sections AB, BD and DE of the beam, respectively, give bending normal stresses as functions of *P* and *z*. Simultaneously substituting in **Equation 25** gives;

$$\sigma_{[0\le z\le 9.5]} = \frac{2(0.5Pz)}{w\left[\frac{1}{6}t^3+2t(c-0.5t)^2\right]} \quad \textbf{(26)}$$

$$\sigma_{[9.5<z\le 13.5]} = \frac{2\left(-0.125Pz^2+2.875Pz-11.281P\right)}{w\left[\frac{1}{6}t^3+2t(c-0.5t)^2\right]} \quad \textbf{(27)}$$

$$\sigma_{[13.5<z\le 23]} = \frac{2(-0.5Pz+11.5P\ )}{w\left[\frac{1}{6}t^3+2t(c-0.5t)^2\right]} \quad \textbf{(28)}$$

In order to determine the required flange width at each position along the beam's *z*-axis, set the bending moment stress in each range to σ_{all} for 0° UD material and isolate *w*;

$$w_{[0\le z\le 9.5]} = \frac{2(0.5Pz)}{\sigma_{all}\left[\frac{1}{6}t^3+2t(c-0.5t)^2\right]} \quad \textbf{(17)}$$

$$w_{[9.5<z\le 13.5]} = \frac{2\left(-0.125Pz^2+2.875Pz-11.281P\right)}{\sigma_{all}\left[\frac{1}{6}t^3+2t(c-0.5t)^2\right]} \quad \textbf{(18)}$$

$$w_{[13.5<z\le 23]} = \frac{2(-0.5Pz+11.5P\ )}{\sigma_{all}\left[\frac{1}{6}t^3+2t(c-0.5t)^2\right]} \quad \textbf{(19)}$$

Since the maximum allowable value of *w* is 4", *t* may be determined by setting *w* equal to 4" in **Equation 17** and solving for *t*. It should be noted that flange widths at the ends of the beam go to zero according to **Equation 18** and **Equation 19**; however, maximum shear forces develop at these locations and the beam must be able to balance on the bottom flanges at its ends. Therefore flange width at the ends should not be below a reasonable recommended value of 2" at the ends of the beam. One may also consider only trimming the top flange to avoid problems with supporting the beam on a narrowed bottom flange. Varying flange width is just one simple way of optimizing the design for its tensile bending strength-to-weight ratio. Other, more complicated ways to lower weight are to vary the flange thickness, the web height, and/or the web thickness.

Appendix C: Manufacturing and Beam Materials

11/2012

FLAXPREG

Description:

FLAXPREG is a range of pre-impregnated material based on an epoxy resin system and pre-treated Flax Fibers using the LINEO patented sizing technology.

Balanced fabric

Unidirectional (UD) fabric

UD fibres

Main markets:		Advantages
Sport and leisure	Flax is already used to improve the dampening properties of rackets, bicycle frames, skis, boards, ...	Dampening properties
Transportation	Already used in aeronautic, automotive, boat manufacturing, railway.	Weight reduction, Mechanical & Acoustic properties, Close to aramid behaviour, Bio-based material
Wind energy	Development projects	Dampening properties, Weight reduction, Bio-based material

Reference	Description	Epoxy part of he total weight	Width
FLAXPREG UD 150	UD fabric - 150gr of flax/m²	50%	1m
FLAXPREG UD 180	UD fabric - 180gr of flax/m²	50%	1m
FLAXPREG BL 150	Balanced fabric - 150gr of flax/m²	50%	1m
FLAXPREG BL 200	Balanced fabric - 200gr of flax/m²	50%	1m
FLAXPREG BL 300	Balanced fabric - 300gr of flax/m²	50%	1m
FLAXPREG BL 550	Balanced fabric - 550gr of flax/m²	50%	1m

Contact: François Vanfleteren – francois.vanfleteren@lineo.eu - +33.232.43.13.67

Appendix C: Manufacturing and Beam Materials

11/2012

Mechanical properties:

Mechanical results from a composite made with 12 layers of "FlaxPreg UD 180":

RATE OF FIBRES	By weigth	65 %
	By volume	60 %
TRACTION (ISO 527)	Tensile strength	330 MPa
	Modulus	35 GPa
	Elongation	1.8 %
FLEXION (ISO 14 125)	Ultimate stress strength	300 MPa
	Modulus	22 GPa
	Elongation	2.4 %
THEORIC DENSITY		1.33 gr/cm³

Dampening properties:

Low frequency dampening (flexion / mode 2):

Product	Dampening ratio
UD Flax	1.47%
UD Carbon	0.18%
UD Glass	0.15%

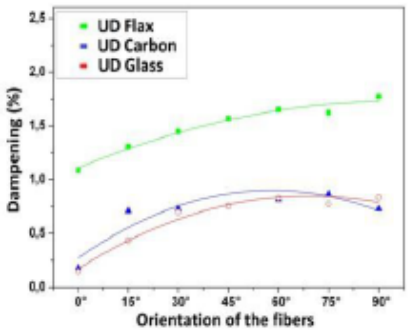

Available curing cycles:

Curing Time	Curing Temperature	*Glass Transition Temperature*
2 hours	110°C	*113°C to 122°C*
1 hour	120°C	*125°C to 134°C*
30 min	130°C	*127°C to 136°C*
1 hour		*135°C to 145°C*
15 min	140°C	*134°C to 144°C*
30 min		*135°C to 145°C*
1 hour		*135°C to 145°C*
15 min	150°C	*128°C to 136°C*
30 min		*136°C to 146°C*

Shelf Life:

Storage Temperature	Shelf Life
< 4°C	> 1 year
23°C	6 – 8 weeks
30°C	3 – 4 weeks

Contact: François Vanfleteren – francois.vanfleteren@lineo.eu - +33.232.43.13.67

Appendix C: Manufacturing and Beam Materials

Nylon Release Peel Ply

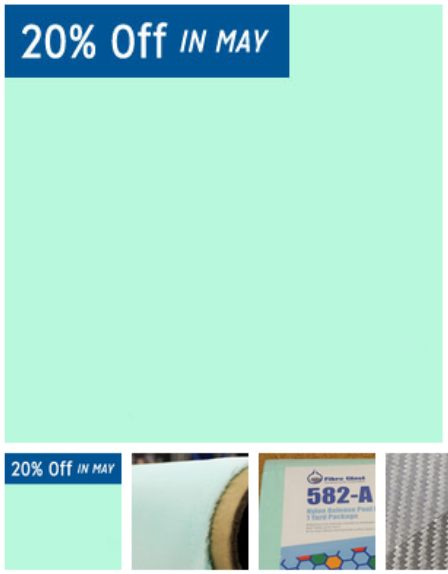

20% Off only in May

Maximum Air and Resin Transfer
This fabric provides an easy release and a textured surface for secondary bonding or painting. Both air and resin will transfer through every pore, ensuring a void-free laminate. Use strips anywhere secondary bonding is to occur. Service temperature is 350 degrees F, 60" wide, and .004" thick. Not recommended for phenolic systems

FIRST QUALITY GUARANTEED

MSDS DATA SHEET

Cut To Length (by yard)

Description	Item #	Price / Yard	Qty	
Cut To Length *min. qty of 10 yds.*	582	~~$8.95~~ $7.15	10	Add to Cart

Quantity Discounts

25+	$6.90
100+	$6.65

Package (pre-cut lengths)

Length	Price/ Roll	Quantity
1 yd Package	~~$12.95~~ $10.35	
3 yd Package	~~$34.95~~ $27.95	
5 yd Package	~~$49.95~~ $39.95	
Swatch (4"x6")	~~$1.95~~ $1.55	

Add to Cart

Appendix C: Manufacturing and Beam Materials

New 7oz Breather and Bleeder Available!
20% Off only in May
Easy to Drape and Binder Free

This high fill non-woven polyester will easily drape and conform closely to the contours of your part. It does not contain any binders which could close off air flow within the mold, and it will readily soak up excess resin.

As a breather, these products are used in the vacuum bagging process to evacuate all of the air in the bag while applying vacuum. A breather allows for even pressure to be applied over the entire surface of the laminate. The breather also allows for any gases produced during the cure to be evacuated from the laminate to your vacuum source. Compared to #579 four ounce, the #1779 seven ounce breather can be used in higher pressure cure cycles and helps to provide a lower amount of surface porosity.

If used as a bleeder, these products absorb excess resin that was applied during the layup process. After the vacuum bagging process is complete, the breather bleeder is simply thrown away. Compared to #579, the #1779 seven ounce breather bleeder will absorb more resin from the laminate which can result in a dry part unless carefully controlled.

If you are working under 40 psi, the #579 is the most commonly selected breather bleeder. If working between 40psi and 85psi, the seven ounce breather is ideal.

Both breather bleeders are 60" wide.

See video for product preview.

FIRST QUALITY GUARANTEED

MSDS DATA SHEET

Cut To Length (by yard)

Description	Item #	Price	Qty
4 oz *min. qty of 10 yds.* Quantity Discounts 25+ $3.45 100+ $3.15	579	~~$4.75~~ $3.80	
7 oz *min. qty of 10 yds.* Quantity Discounts 25+ $5.85 50+ $5.55 100+ $5.15	1779	~~$7.75~~ $6.20	

Add to Cart

Package / Roll (pre-cut lengths)

Length	Price/ Roll	Quantity
4 oz - 1 yd Package	~~$7.95~~ $6.35	
4 oz - 3 yd Roll	~~$16.95~~ $13.55	
4 oz - 5 yd Roll	~~$24.95~~ $19.95	
4 oz - Swatch (4"x6")	~~$1.95~~ $1.55	
7 oz - 1 yd Roll	~~$10.95~~ $8.75	
7 oz - 3 yd Roll	~~$24.95~~ $19.95	
7 oz - 5 yd Roll	~~$39.95~~ $31.95	
7 oz - (4"x6") Swatch	~~$1.95~~ $1.55	

Add to Cart

Appendix C: Manufacturing and Beam Materials

Stretchlon 200 Bagging Film

New 60"/120" Wide Centerfold Available!
20% Off only in May
Available in 60" wide sheet, or 120" wide centerfolds.

Stretchlon 200 is ideal because it is able to stretch to compress every area of the mold. This high elongation vacuum bagging film is rated for temperatures up to 250°F and can stretch to 500% of its original length. Unlike traditional bagging film, Stretchlon can be fitted over complex shapes without pleats or rabbit ears as it stretches to conform to nearly every shape. This material can conform to autoclave pressures.

Compared to Stretchlon 800, the 200 is a thinner material and can be stretched to a larger amount of its original length. Compatible with epoxy resin only.

See video for product preview.

Stretchlon® is a registered trademark of Airtech International.

FIRST QUALITY GUARANTEED

MSDS DATA SHEET

Cut To Length (by yard)

Description	Item #	Price	Qty
60" Wide Sheet *min. qty of 10 yds.* Quantity Discounts 25+ $2.80 50+ $2.60 100+ $2.35 667+ $2.10	1678	~~$3.90~~ $3.10	
60"/120" Wide Centerfold *min. qty of 10 yds.* Quantity Discounts 25+ $5.70 50+ $5.45 100+ $5.20 333+ $5.00	1778	~~$7.45~~ $5.95	

Add to Cart

Roll (pre-cut lengths)

Length	Price/ Roll	Quantity
60" Wide Sheet - 1 yd Roll	~~$4.95~~ $3.95	
60" Wide Sheet - 3 yd Roll	~~$13.95~~ $11.15	
60" Wide Sheet - 5 yd Roll	~~$19.95~~ $15.95	
60"/120" Centerfold 1 yd Roll	~~$9.95~~ $7.95	
60"/120" Wide Centerfold 3 yd Roll	~~$27.95~~ $22.35	
60"/120" Wide Centerfold 5 yd Roll	~~$39.95~~ $31.95	
Swatch (4"x6")	~~$1.95~~ $1.55	

Add to Cart

Appendix C: Manufacturing and Beam Materials

Gray Sealant Tape

Description	Item #	Price	Qty
Single Roll	581-A	~~$7.95~~ $6.35	
Case (40 Rolls)	581-B	~~$259.95~~ $207.95	

Quantity Discounts
9+ $159.95

Add to Cart

20% Off only in May

Leak Free
This tape will seal the bag to aluminum, steel, fiberglass, nickel, and graphite tool surfaces yet strips easily after cure. Use to plug leaks and tears in the bag that can develop during cure. Maximum service temperature is 400 degrees F. 1/2" wide, 1/8" thick, and 25' per roll.

MSDS DATA SHEET

Vacuum Connector

Description	Item #	Price	Qty
Vacuum Connector (each)	891-A	$4.95	
Vacuum Connector (dozen)	891-B	$49.95	

Add to Cart

View Larger

This 1/2" ID connector is all that is required to complete a basic installation. Place the connector through the bag, attach tubing, and you're ready to begin!